Meteoritics & Planetary Science 39, Nr 4, 503–529 (2004)
Abstract available online at http://meteoritics.org

Petrogenesis of lunar highlands meteorites: Dhofar 025, Dhofar 081, Dar al Gani 262, and Dar al Gani 400

J. T. CAHILL,[1, 2*] C. FLOSS,[3] M. ANAND,[1] L. A. TAYLOR,[1] M. A. NAZAROV,[4] and B. A. COHEN[5]

[1]Planetary Geosciences Institute, Department of Earth and Planetary Sciences, University of Tennessee, Knoxville, Tennessee 37996, USA
[2]Hawaii Institute of Geophysics and Planetology, University of Hawaii, Honolulu, Hawaii 96822, USA
[3]Laboratory for Space Sciences, Washington University, St. Louis, Missouri 63130, USA
[4]Vernadsky Institute of Geochemistry and Analytical Chemistry, Russian Academy of Sciences, Moscow 117975, Russia
[5]Department of Earth and Planetary Sciences MSCO3–2040, University of New Mexico, Albuquerque, New Mexico 87131–0001, USA
*Corresponding author. E-mail: jcahill@higp.hawaii.edu

(Received 14 November 2002; revision accepted 1 March 2004)

Abstract–The petrogenesis of four lunar highlands meteorites, Dhofar 025 (Dho 025), Dhofar 081 (Dho 081), Dar al Gani 262 (DaG 262), and Dar al Gani 400 (DaG 400) were studied. For Dho 025, measured oxygen isotopic values and Fe-Mn ratios for mafic minerals provide corroboratory evidence that it originated on the Moon. Similarly, Fe-Mn ratios in the mafic minerals of Dho 081 indicate lunar origin.

Lithologies in Dho 025 and Dho 081 include lithic clasts, granulites, and mineral fragments. A large number of lithic clasts have plagioclase AN# and coexisting mafic mineral Mg# that plot within the "gap" separating ferroan anorthosite suite (FAN) and high-magnesium suite (HMS) rocks. This is consistent with whole rock Ti-Sm ratios for Dho 025, Dho 081, and DaG 262, which are also intermediate compared to FAN and HMS lithologies. Although ion microprobe analyses performed on Dho 025, Dho 081, DaG 262, and DaG 400 clasts and minerals show far stronger FAN affinities than whole rock data suggest, most clasts indicate admixture of ≤12% HMS component based on geochemical modeling. In addition, coexisting plagioclase-pyroxene REE concentration ratios in several clasts were compared to experimentally determined plagioclase-pyroxene REE distribution coefficient ratios. Two Dho 025 clasts have concordant plagioclase-pyroxene profiles, indicating that equilibrium between these minerals has been sustained despite shock metamorphism. One clast has an intermediate FAN-HMS composition.

These lunar meteorites appear to represent a type of highland terrain that differs substantially from the KREEP-signatured impact breccias that dominate the lunar database. From remote sensing data, it is inferred that the lunar far side appears to have appropriate geochemical signatures and lithologies to be the source regions for these rocks; although, the near side cannot be completely excluded as a possibility. If these rocks are, indeed, from the far side, their geochemical characteristics may have far-reaching implications for our current scientific understanding of the Moon.

INTRODUCTION

Despite contributions from the Apollo and Luna missions, two-thirds of the mare regions and the entire far side of the Moon are not represented in the lunar database (Pieters 1978). Furthermore, Clementine and Lunar Prospector remote sensing data indicate that the near and far sides are substantially different in terms of inferred chemical composition and lithologies (Spudis et al. 2000, 2002). Thus, it is likely that our understanding of the lunar geologic processes and history is incomplete. However, newly discovered lunar meteorites could potentially supply the samples necessary to characterize previously unsampled terrains of the Moon. Recent meteorite finds from the Dhofar region of Oman (which account for nearly half of the 30 known lunar meteorites) may represent such samples.

In this study, we have examined the mineralogy and petrology of the four highland breccia meteorites Dhofar 025 (Dho 025), Dhofar 081 (Dho 081), Dar al Gani 262 (DaG 262), and Dar al Gani 400 (DaG 400). We have used geochemical (major, minor, and trace element) analyses of bulk rock and individual mineral grains to: 1) provide

evidence for the lunar origin of these rocks; 2) distinguish between mare and highland clasts; 3) identify the clasts least affected by shock metamorphism; 4) infer near or far side origins for these rocks; and 5) determine how this information can further improve our current understanding of the Moon.

ANALYTICAL TECHNIQUES

Thin sections of each meteorite were examined with an optical microscope using transmitted and reflected light. Major and minor element mineral compositions of plagioclase, olivine, and pyroxene in Dho 025 and Dho 081 were determined on a fully automated CAMECA SX-50 electron microprobe at the University of Tennessee using an accelerating voltage of 15 kV. For plagioclase analyses, a beam current of 20 nA and a spot size of 5 μm was used. Other minerals were analyzed with a beam current of 30 nA and a 2 μm spot size. The counting times were 20 sec for all elements analyzed in plagioclase and 30 sec for elements in all other minerals. Standard online matrix corrections (PAP) were applied to all analyses.

The oxygen isotopic composition of Dho 025 was determined at the University of Chicago. Separate splits weighing ~10 mg were analyzed using the procedure outlined by Clayton and Mayeda (1983, 1996). The whole rock chemical composition of Dho 025 was determined at the Vernadsky Institute, Moscow, Russia. An aliquot of a 1-g sample was powdered in an agate mortar to obtain homogeneous material for whole rock analyses. Silicon, Ti, Al, Cr, Fe, Mn, Mg, and Ca were determined by XRF and ICP. Sodium and K were measured by atomic absorption. Trace elements were analyzed by instrumental neutron activation analysis (INAA).

Minor and trace element (including REE) concentrations were determined for selected mineral grains and clasts in Dho 025, Dho 081, DaG 262, and DaG 400 using the modified CAMECA IMS 3f ion-microprobe at Washington University, St. Louis following the methods outlined by Zinner and Crozaz (1986a). Analyses were obtained using an O^- beam with an accelerating voltage of 12.5 kV. Secondary ions were collected at low mass resolution using energy filtering (100 V offset) to remove complex molecular interferences. Simple interferences not removed by this method were corrected by deconvolution of major molecular interferences in the mass regions K-Ca-Ti, Rb-Sr-Y-Zr, and Ba-REEs (Alexander 1994). Concentrations were obtained using sensitivity factors reported by Floss and Jolliff (1998), Hzu (1995), and Zinner and Crozaz (1986b) for the REE and by Hsu (1995) for other elements. All mineral analyses were normalized to the reference element, Si, using SiO_2 concentrations determined by electron microprobe.

Polymineralic clast analyses were normalized using an SiO_2 concentration of 50 wt%, a value that should be fairly representative of the average SiO_2 concentrations of the clasts, based on the abundances of the minerals present (plagioclase, pyroxene, and olivine) and their average SiO_2 concentrations (44 wt%, 50 wt%, and 35 wt%, respectively). This approach may overestimate the trace element concentrations of clasts with high proportions of plagioclase and olivine, but the effect should be less than 15% in most clasts. Some error may also be introduced by the fact that different minerals in the matrices of polymineralic clasts have different ion yields, but it is difficult to estimate the magnitude of this effect. However, we note that the difference in relative sensitivity factors between various REE is <30% for a wide variety of standards (including oxides, silicates, and glass) and, thus, relative REE concentrations (i.e., the shapes of the patterns) are not affected by this approach.

PETROGRAPHY AND MINERAL CHEMISTRY

Dho 025, an anorthositic regolith breccia weighing 751 g, was found in Dhofar, Oman in January of 2000 (Grossman 2000). Dho 081, a shocked, feldspathic fragmental highlands breccia, was discovered a year earlier. The cosmogenic exposure age for Dho 025 is between 13–20 Myr (Nishiizumi et al. 2002). However, for Dho 081, the transition time between the Moon and the Earth was too short for detectable amounts of long-lived nuclides to be produced (Nishiizumi et al. 2002). The lithologies present in these two meteorites include: 1) lithic clasts, 2) granulites, and 3) mineral fragments. A summary of clast types and their mineral compositions is listed in Table A1.

Lithic clasts are the dominant lithology in Dho 025 (Figs. 1a–1b). These clasts are partially recrystallized monomict and polymict rocks with anorthositic to troctolitic-anorthosite compositions. Monomict rocks consist of single-crystal plagioclase with subhedral to spherical mafic inclusions (Figs. 1c–1d), similar to rocks from North Ray Crater (Norman 1981). These clasts are 100–200 μm in size and are predominantly plagioclase (AN# 96–98) with olivine inclusions of homogenous composition (Fo 69–80). Polymict rocks range from recrystallized anorthosites to microporphyritic crystalline melt-rocks. They consist mainly of plagioclase (AN# 94–98), with minor amounts of mafic minerals (Mg# 64–83) (Fig. 2a). Mafic minerals in these clasts have subhedral shapes due to interaction with an impact melt.

Only one granulitic troctolite clast was observed in Dho 025 (Fig. 1e). It has a granoblastic texture (Cushing et al. 1999) and consists of plagioclase (AN# 96) and olivine (Fo 79) grains. Mineral fragments (Fig. 1f) present in the breccia matrix include plagioclase (AN# 95–98), orthopyroxene (Mg# ~75), pigeonite (Mg# 65–69), and augite (Mg# 66–80). Accessory minerals include spinel, ilmenite, FeNi metal, troilite, and silica. Akaganéite (β-FeOOH) occurs as rims on FeNi metal grains and is most likely of terrestrial origin. Other terrestrial alteration products (calcite, celestite, and gypsum) are also present in the meteorite, mainly filling cracks.

Compared to Dho 025, Dho 081 is poor in mafic mineral

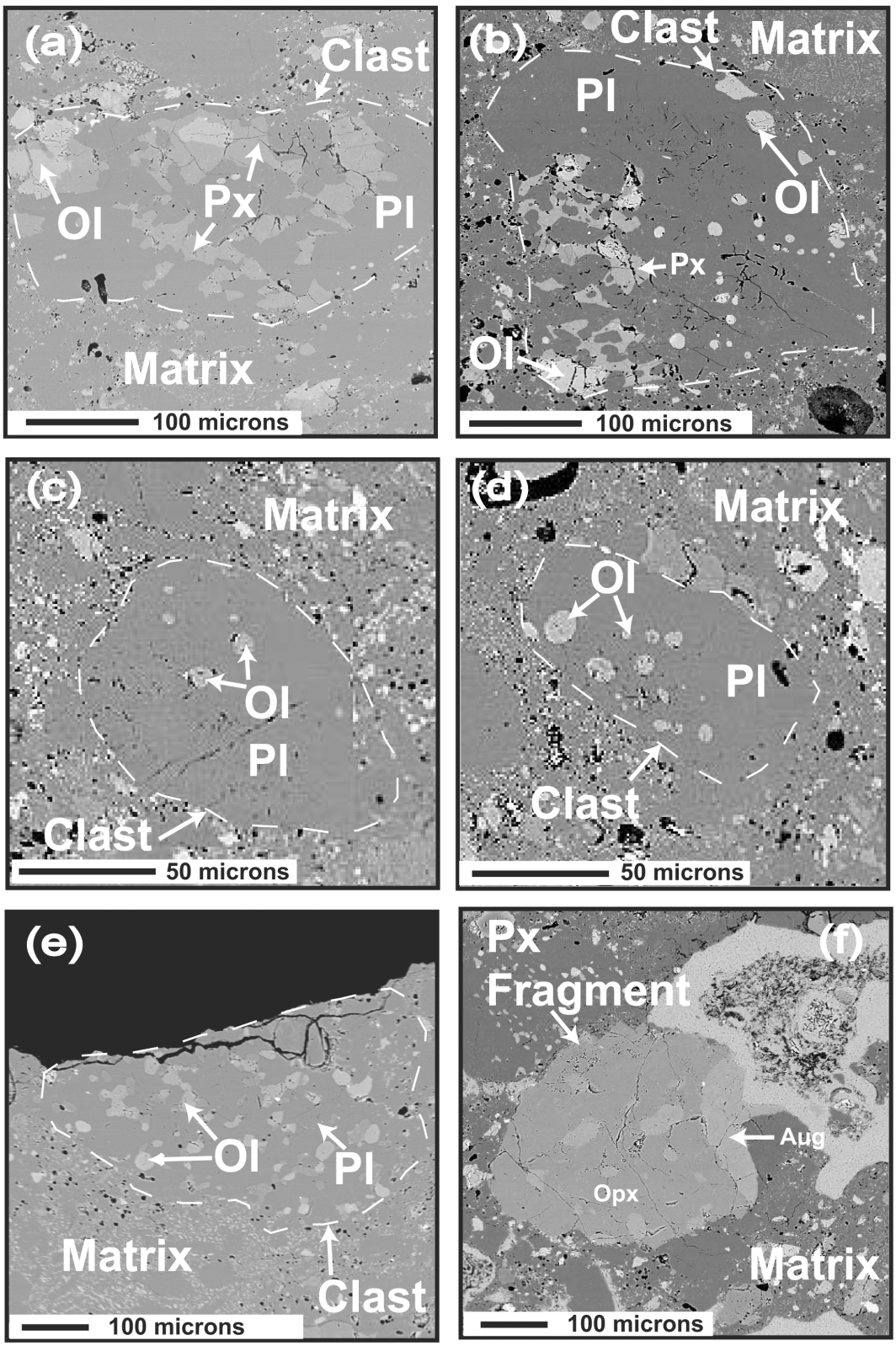

Fig. 1. Backscattered electron images of lunar meteorite Dho 025: a and b) lithic clasts with embayed mafic minerals resulting from interaction with impact melt. These clasts are surrounded by a fine-grained and glassy meteorite matrix; c and d) two single-crystal plagioclase clasts with spherical olivine inclusions; e) granulite clast consisting of plagioclase and olivine mineralogy and exhibiting a granoblastic texture; f) bimineralic pyroxene fragment consisting of augite and orthopyroxene.

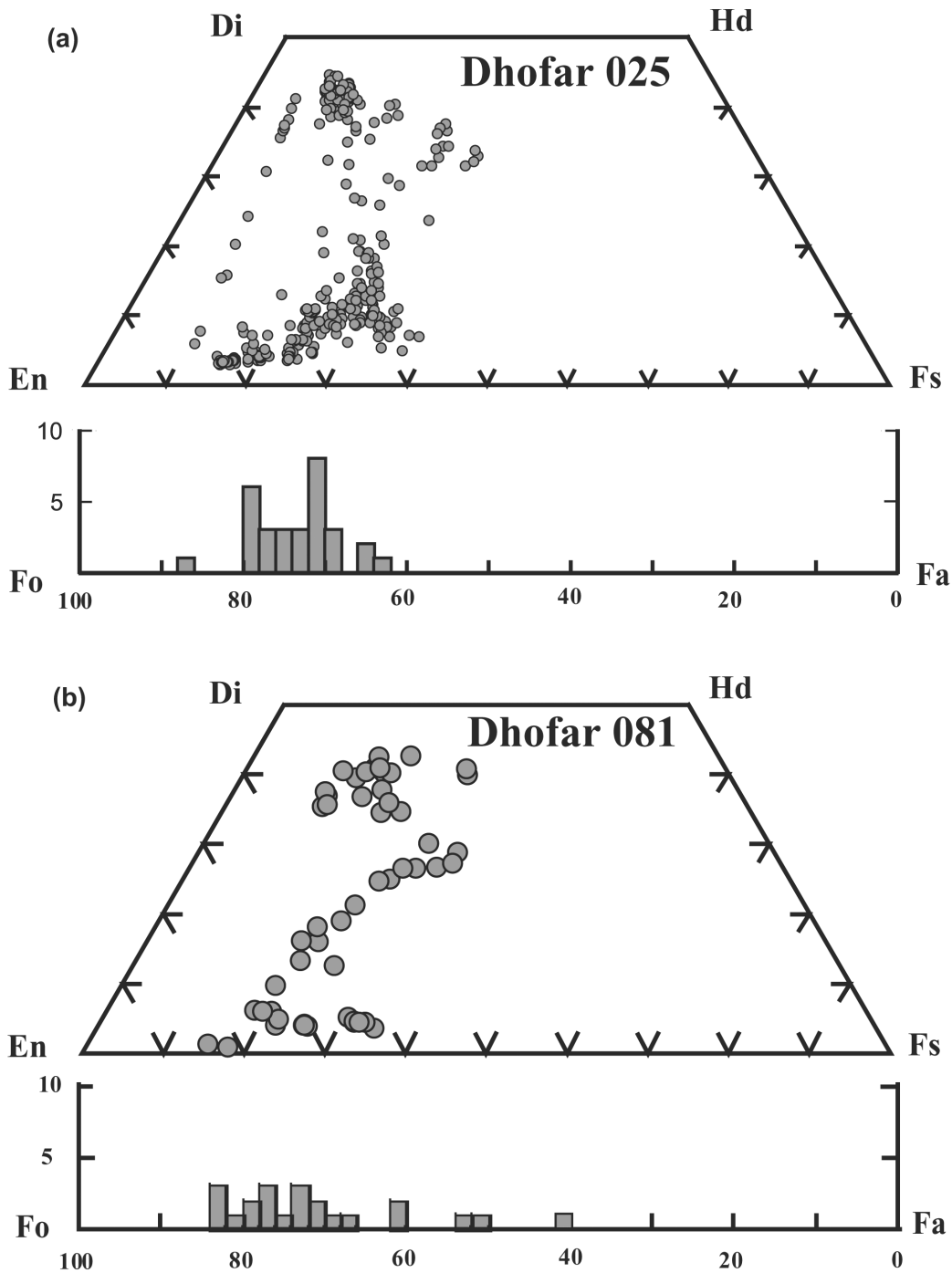

Fig. 2. Pyroxene and olivine major element compositions for lunar meteorites (a) Dho 025 and (b) Dho 081.

constituents. Lithic clasts in this breccia are partially recrystallized anorthosites that dominantly consist of plagioclase (AN# 94–97), with embayed and/or zoned mafic minerals (Figs. 3a–3c). Olivine is the most abundant mafic mineral (Fo 56–83), while pyroxene (Mg# 58–78) is a minor constituent in these clasts (Fig. 2b). Granulite lithologies in Dho 081 range from 200–500 μm in size and have granoblastic textures (Fig. 3d). Though consisting mostly of plagioclase (AN# 96–97), these clasts also contain fine-grained olivines with compositions of Fo 70–75. The majority of Dho 081 clasts are individual mineral fragments (Figs. 3e–3f). Plagioclase fragments (AN# 94–98) are most abundant, while mafic mineral fragments are mainly olivine, often with pyroxene rims. Olivine fragments commonly exhibit reverse zoning (e.g., core: Fo ~71 versus rim: Fo ~80). One olivine grain (~350 μm; Fig. 3e) in particular is characterized by a

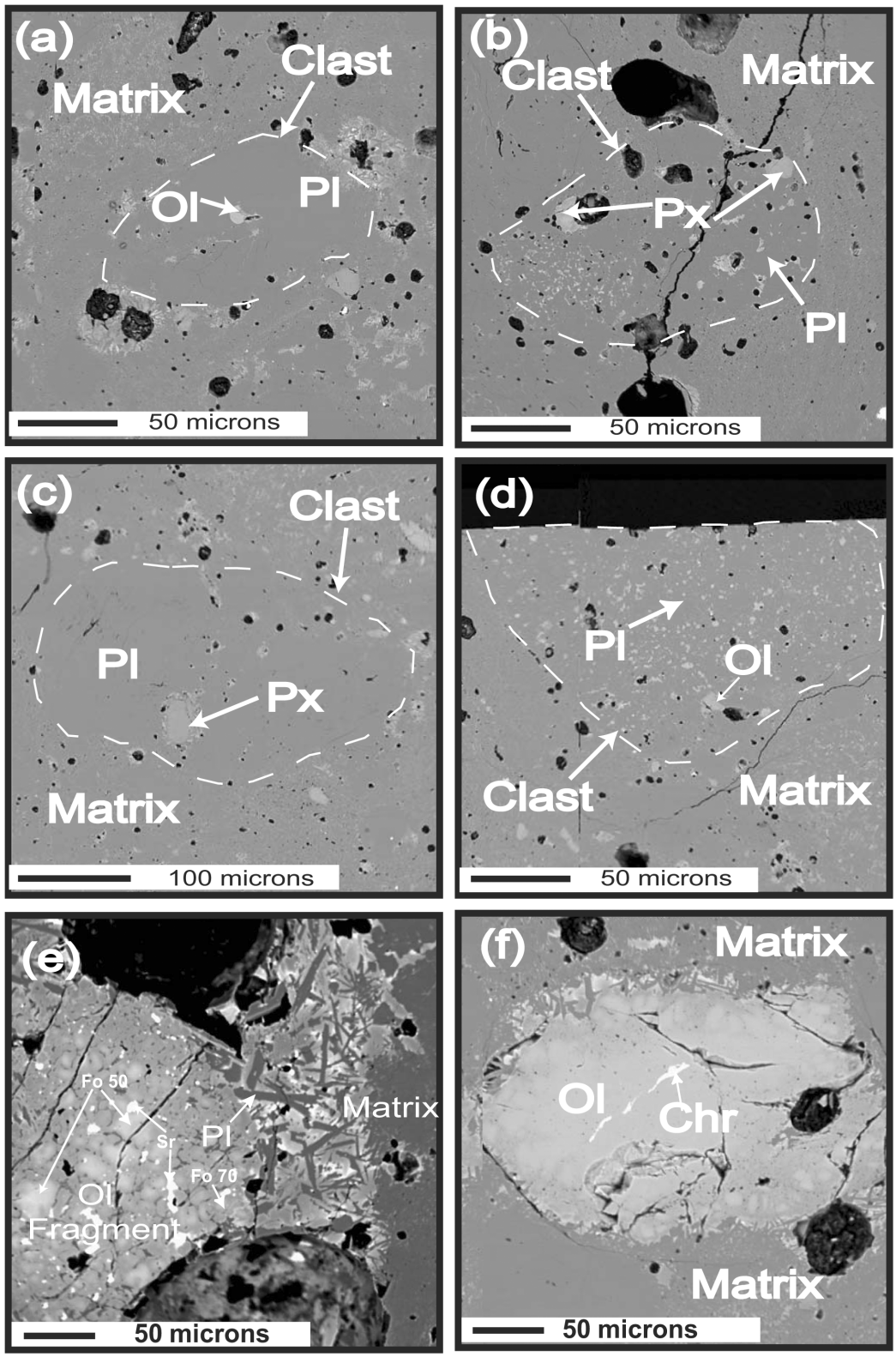

Fig. 3. Backscattered electron images of lunar meteorite Dho 081: a–c) mafic-poor lithic clasts; d) granoblastic granulite with fine-grained olivine mineralogy; e) backscattered electron image of a heavily melted and embayed relic olivine mineral fragment with several vesicles in and around the edges. This olivine fragment has reverse zonation (core: Fo ~50; rims: Fo ~70) probably due to re-equilibration with the impact melt matrix; f) olivine mineral fragment with chromite vein.

compositional variance of Fo ~20 from core to rim (i.e., Fo ~50 to Fo ~70). Reverse zoning is likely due to interaction with an impact melt. Monomineralic pyroxene grains are also compositionally variable (Mg# 41–72). Accessory minerals in the meteorite matrix include Cr-spinel, Ti-chromite, and troilite.

Lunar meteorites DaG 262 and DaG 400 are also anorthositic breccias (Bischoff et al. 1998; Zipfel et al. 1998). In the present study, we have only made trace element measurements in a number of DaG 262 and DaG 400 clasts. Bischoff et al. (1998) carried out a detailed characterization of the types of clasts present in DaG 262 and their mineral chemistries and note that this meteorite is dominated by feldspathic, fine-grained to microporphyritic crystalline melt clasts. Granulitic clasts, as well as recrystallized and cataclastic anorthosites, are also present, but mafic mineral-rich clasts are rare. Plagioclase is highly anorthitic (AN# ≥95), and mafic minerals (olivine and pyroxene) have Mg#s ranging from 50 to 70 (Jolliff et al. 1999), suggesting an affinity to the ferroan anorthosite (FAN) suite for much of the material in this meteorite. Similarly, DaG 400 is dominated by anorthositic clasts, most of which are fine-grained to microporphyritic impact melt clasts (Zipfel et al. 1998). Recrystallized anorthosites, granulites, and mineral fragments are also present, but as in DaG 262 and Dho 081, mafic lithologies are rare. Plagioclase in all DaG 400 lithologies ranges from AN 94–98 (Semenova et al. 2000). Mafic minerals associated with anorthosites (which make up 95% of all clasts) have more ferroan compositions (in the FAN range) than anorthositic norites and troctolites, which fall in the FAN-high magnesium suite (HMS) "gap" (Semenova et al. 2000).

Like DaG 400, Dho 025 and Dho 081 have lithologies with strong FAN affinities, but some clasts plot within the FAN-HMS gap (Figs. 4 and 5). Traditionally, pristine Apollo and Luna rocks, as well as other lunar meteorites have plotted within the FAN and HMS envelopes. Rocks that plot in between (i.e., in the FAN-HMS gap) have been classified under the general term "lunar granulites" (Bickel and Warner 1978; Lindstrom and Lindstrom 1986; Norman 1981). Several other recent characterizations of minerals in lunar meteorites have revealed clast compositions plotting regularly in this gap but without textures typical of granulites (Cushing et al. 1999). Meteorites that display these gap compositions without characteristic granulitic textures include three of the four lunar meteorites in this study (DaG 400, Dho 025, and Dho 081) and several other Dhofar meteorites (Dho 280, Dho 301, Dho 302, and Dho 303) (Anand et al. 2002; Nazarov et al. 2002; Semenova et al. 2000). Since the clasts in these meteorites show neither pristine nor granulitic textures, we have classified them as mixed impactites. This designation denotes the possibility that these clasts are mixtures of FAN and HMS components created by impact melting. However, the possibility exists that these clasts may retain information from pristine crustal

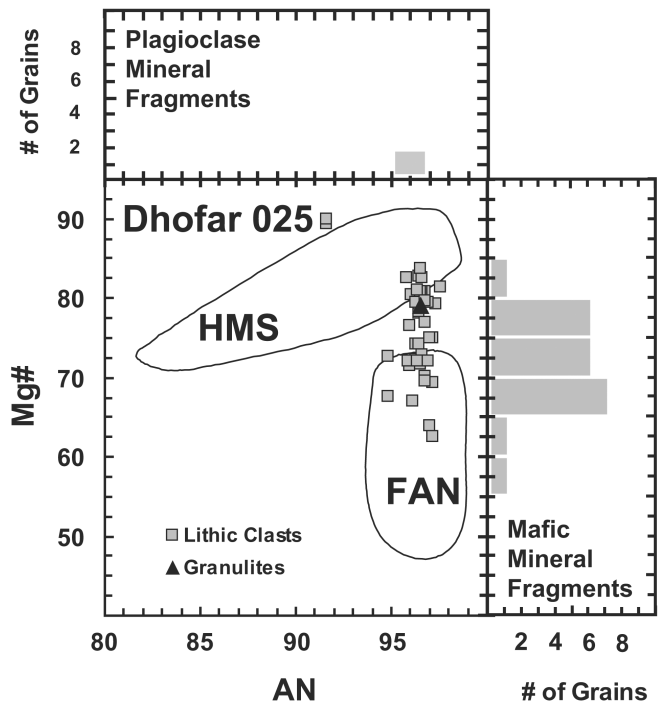

Fig. 4. Mafic phase (olivine and pyroxenes) Mg# versus AN# in plagioclase for Dho 025 clasts. Compositional fields for FAN and HMS rock suites are shown for comparison (Warren 1985). Mg# for mafic mineral fragments that lack coexisting plagioclase grains are shown on the right portion of the diagram, and AN# for plagioclase fragments lacking coexisting mafic mineral grains are shown on the top portion of the diagram.

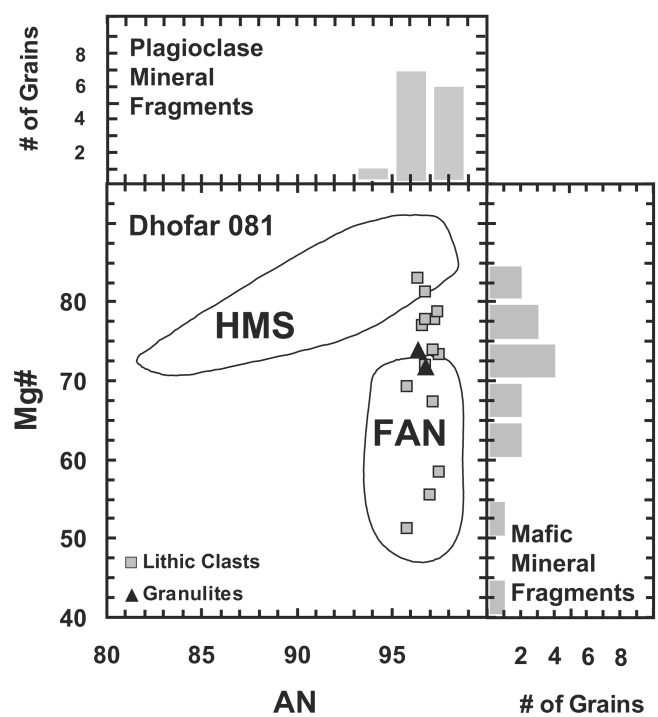

Fig. 5. Mg# versus AN# plot for Dho 081 clasts. The symbols and fields are the same as in Fig. 4.

lithologies. Therefore, both possibilities were investigated further using whole rock, clast, and mineral composition data.

EVIDENCE FOR LUNAR ORIGIN

Fe-Mn Ratios

It is well known that Fe and Mn distributions in some minerals are diagnostic of their parent bodies (Laul et al. 1972). Conditions of the initial accreted material, the extent of core formation, and the oxygen fugacity of a particular body constrain the Fe-Mn ratios of the parent body (Papike 1998). In the case of the Moon, an additional factor affecting Fe-Mn distributions among minerals may have been the loss of relatively volatile Mn during the Moon-forming impact event (Papike 1998; Papike et al. 2003).

Figure 6 shows the Fe-Mn ratios of olivines and pyroxenes from Dho 025 and Dho 081. Although olivines from both meteorites plot along the lunar trend, pyroxenes appear to have slightly elevated Mn with average pyroxene Fe-Mn ratios in Dho 025 and Dho 081 of 49.7 and 52.3, respectively. These observations may indicate that fractionation of Fe and Mn in olivine differs slightly from that of pyroxene. However, this is difficult to determine considering the low concentrations of both Fe and Mn in these minerals. A simpler explanation may be that the observed variations are due to the difference in lithologies analyzed in this study compared to that by Papike (1998) (i.e., anorthosite versus basalt), which established the basis for such discriminations. Differences between these two rock types in starting bulk composition or subsequent crystallization sequences may account for the elevated levels of Mn. Nonetheless, the average Fe-Mn ratios in the olivine and pyroxene of Dho 025 and Dho 081 (86.0 and 87.9, respectively) are consistent with Apollo and Luna rocks. Furthermore, the whole rock Fe-Mn ratio for Dho 025 is 65.7, similar to the lunar meteorite average of 70 (Palme et al. 1991).

Oxygen Isotopes

The Dho 025 oxygen isotope composition is $\delta^{18}O$ = +5.47‰ and $\delta^{17}O$ = +2.81‰ (Taylor et al. 2001). This composition lies along the terrestrial-lunar fractionation line (TLFL) (Fig. 7) and is consistent with results for other lunar meteorites including DaG 262 and DaG 400. In addition, the oxygen isotope data also agree with those of Apollo mare basalts and highlands rocks. Minor deviations from the TLFL are attributed to desert weathering influences (Stelzner et al. 1999).

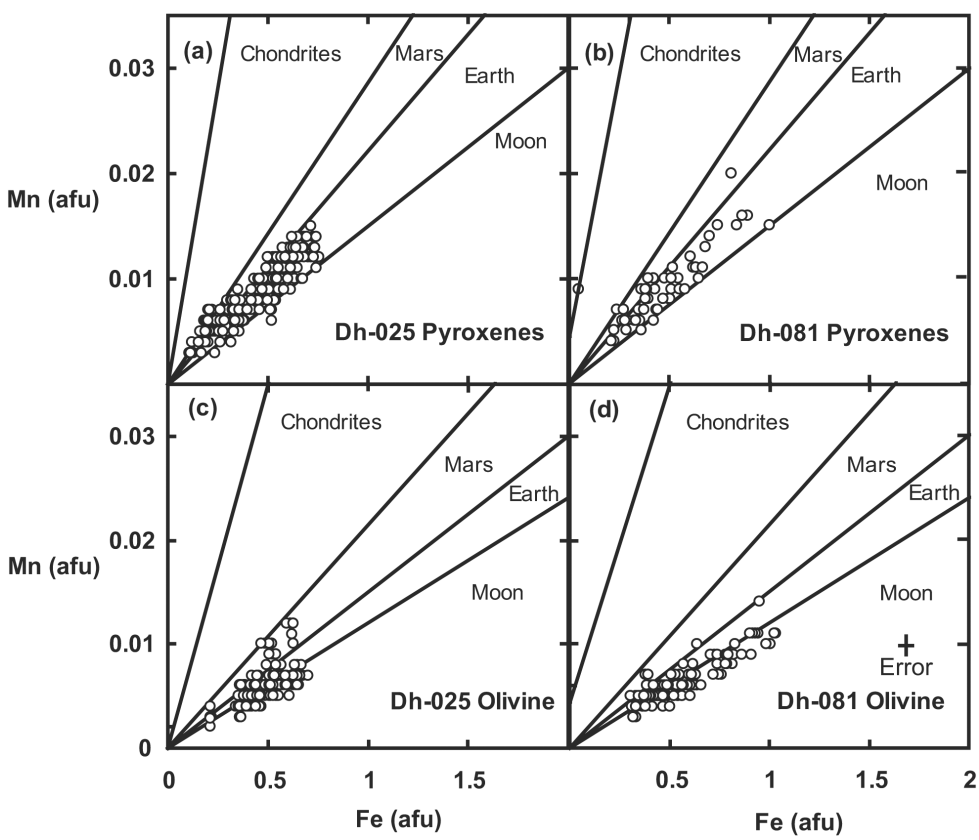

Fig. 6. Fe-Mn ratios for Dho 025 and Dho 081: a and b) pyroxene; c and d) olivine. The Fe-Mn ratios in olivines are typical of lunar rocks. However, the Mn concentrations in pyroxenes for both Dho 025 and Dho 081 are slightly elevated. The Fe-Mn trends for various planetary bodies are from Papike (1988) and Papike et al. (2003).

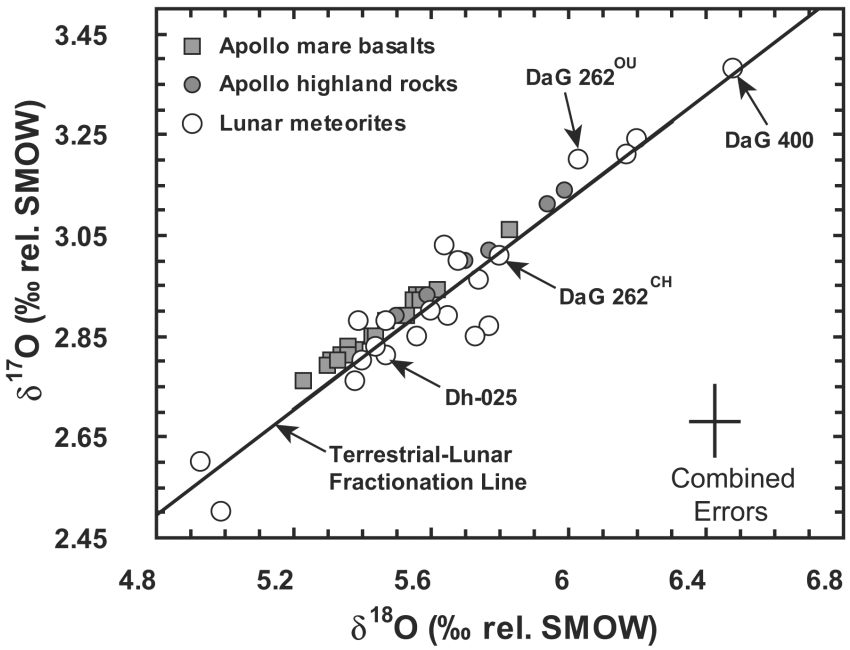

Fig. 7. The oxygen isotopic composition of Dho 025 compared to other lunar meteorites, Apollo mare basalts, and Apollo highland rocks (Arai and Warren 1999; Clayton and Mayeda 1983, 1996; Fagan et al. 2000, 2001a; Kaiden and Kojima 2002; Kojima and Imae 2001; Wiechert et al. 2001). Data for DaG 262 and 400 were reported by Bischoff et al. (1998) and Zipfel et al. (1998), respectively. One analyses of DaG 262 was made at Chicago University (CH) and one at Open University (OU).

WHOLE ROCK COMPOSITIONS

The whole rock composition of Dho 025 was compared to those of Dho 081, DaG 262, DaG 400, other lunar highlands and mare meteorites, as well as Apollo samples (Table 1). Most of the known lunar meteorites (~80%) are breccias or impact melts with highlands characteristics (e.g., Dho 026, MAC 88104/5, Y-86032, Y-82192, ALH A81005, Y-791197, and QUE 93069). However, some lunar meteorites (e.g., Dho 287, QUE 94281, Y-793272, Y-981031, EET 87521, EET 96008, A-881757, and NWA 032) contain substantial mare basalt components. Highlands rocks and mare basalts can have similar trends on Mg# versus AN# plots, but they can be distinguished by their Fe-Sc ratios (Palme et al. 1991). Figure 8 shows that Dho 025, Dho 081, DaG 262, and DaG 400 have similar Fe-Sc ratios, close to the typical highland average of ~4000.

Figure 9 compares Dho 025, Dho 081, DaG 262, DaG 400, and other lunar highland meteorites with highlands regolith samples from the Apollo 14 and 16 sites (Korotev 1997; Warren and Wasson 1980). Using these diagrams, the relative proportions of modal pyroxene (Sc, Sm) and plagioclase (Al_2O_3) can be inferred. Dho 025, Dho 081, DaG 262, and DaG 400 have similar concentrations of Sc and Al_2O_3 to Apollo 16 regolith breccias (Fig. 9a). In contrast, all lunar highlands meteorites have systematically depleted Sm concentrations (by a factor of 10) compared to Apollo 14 and 16 highlands regolith (Fig. 9b). Thus, these data suggest that although these meteorites are composed of highlands material, they are compositionally different from the Apollo and Luna highlands regolith samples collected to date. The large compositional separation between Apollo regolith breccias and lunar meteorites, in Fig. 9b, suggests that these meteorites represent a distinct compositional suite. Considering their highly anorthositic nature and the apparent lack of KREEP, these meteorites may represent a type of crustal terrain that differs significantly from the KREEPy impact melt breccias that are prevalent in the Apollo collection. Because of these readily apparent differences, the highland regions of the lunar far side appear to be likely candidates for the source areas of these rocks. However, it is also possible that a previously unsampled KREEP-poor highland terrain on the lunar near side is the source region for these meteorites. In either case, these lunar meteorites represent new lithological variants in the lunar database and may provide additional clues about the genetic history of the Moon.

Dho 025 has a lower Al_2O_3 concentration (26.1 wt%) compared to most other lunar highlands meteorites. In contrast, Dho 081 and DaG 400 have the highest concentrations of Al_2O_3 (30.5 and 29.2 wt%, respectively) and, thus, are consistent with having the largest modal percentage of plagioclase relative to other lunar meteorites. These two meteorites represent the most anorthositic compositions of all lunar highlands meteorites reported to date (Fig. 9a).

Dho 025, Dho 081, DaG 262, and DaG 400 have low concentrations of Na, Th, Ti, and other incompatible elements compared to typical Apollo 14 and 16 highlands regolith

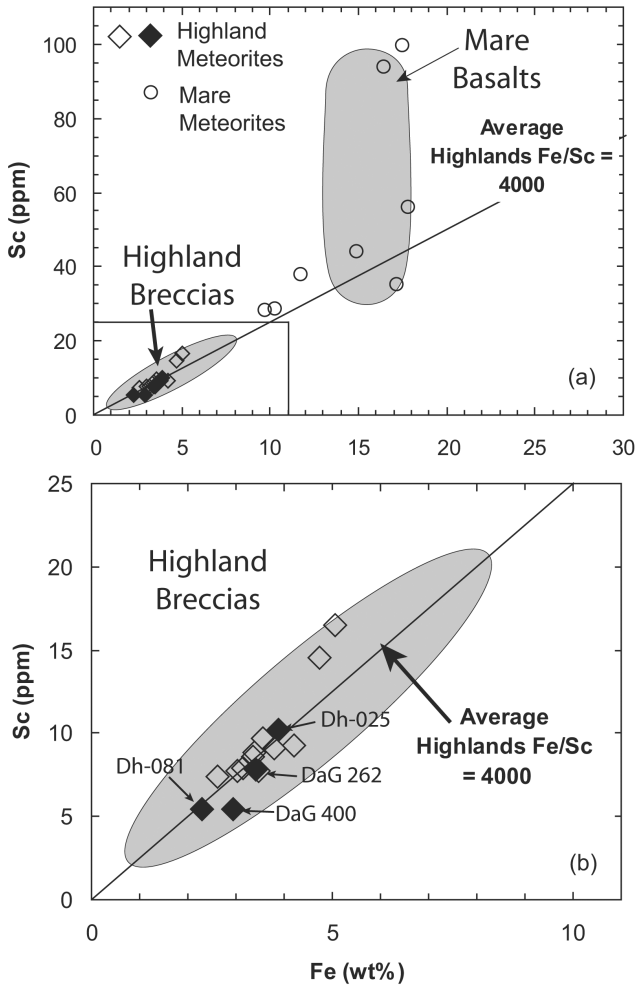

Fig. 8. Whole rock Fe versus Sc easily distinguishes mare and highland lithologies: a) mare and mixed lithologies (Dho 287, QUE 94281, Y-793272, Y-981031, EET 87521, EET 96008, A-881757, and NWA 032) are shown as open circles (Anand et al. 2003; Demidova et al. 2002; Fagan et al. 2001b; Jolliff et al. 1998; Koeberl et al. 1991b; Lindstrom et al. 1991; Snyder et al. 1999; Warren and Kallemeyn 1989, 1993); b) enlarged view of the highland breccia suite. The filled diamonds are lunar highland meteorites Dho 025, Dho 081, DaG 262, and DaG 400 (Bischoff et al. 1998; Warren et al. 2001; Zipfel et al. 1998). The open diamonds represent highland meteorites from other studies (Dho 026, MAC 88104/5, Y-86032, Y-82192, ALH A81005, Y-791197, and QUE 93069) (Cohen et al. 2003; Koeberl et al. 1991a; Korotev et al. 1996; Neal et al. 1991; Palme et al. 1991; Semenova et al. 2000; Spettel et al. 1995).

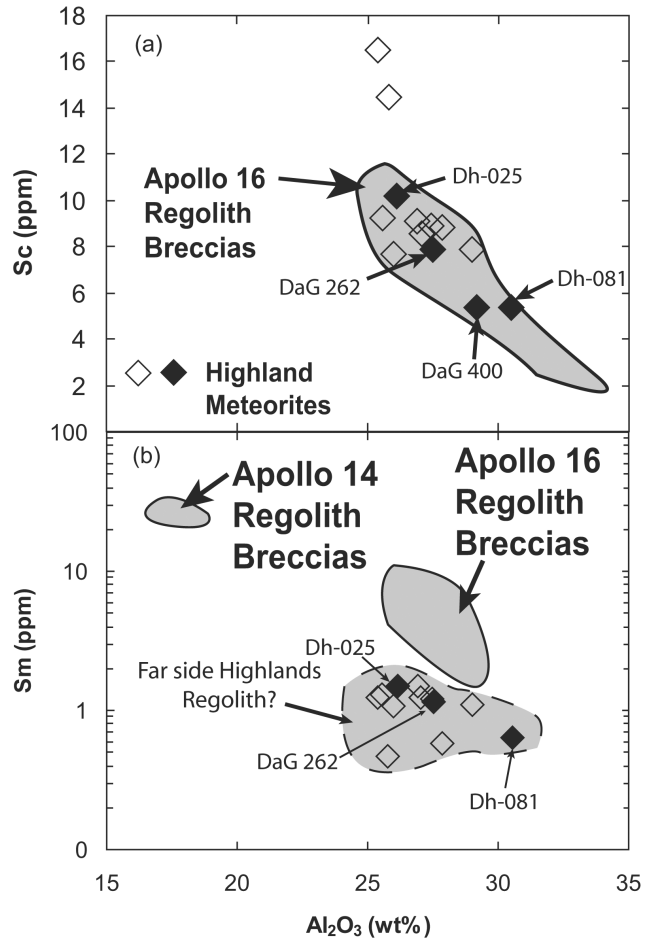

Fig. 9. Whole rock Sc and Sm versus Al_2O_3 in lunar meteorites: a) Apollo 16 regolith compositional envelope (Korotev 1997) is shown for comparison; b) compositional envelopes for Apollo 14 and Apollo 16 regoliths (Warren and Wasson 1980) are shown for comparison. Lunar highlands meteorites Dho 025, Dho 081, and DaG 262 are shown as filled diamonds (Bischoff et al. 1998; Warren et al. 2001; Zipfel et al. 1998). Other lunar highland meteorites are shown as open diamonds (Cohen et al. 2003; Koeberl et al. 1991a; Korotev et al. 1996; Neal et al. 1991; Palme et al. 1991; Semenova et al. 2000; Spettel et al. 1995).

breccias but have concentrations similar to those of other lunar meteorites (Table 1). Siderophile element (Re, Os, Ir, and Au) abundances in Dho 025 are similar to other highlands meteorites, but Dho 081 is depleted (Bischoff et al. 1998; Palme et al. 1991).

Compared to other FAN, HMS, and KREEP rocks (Taylor 1982), Dho 025, Dho 081, and DaG 262 have intermediate Ti-Sm ratios (Fig. 10). All highlands meteorites (with the exception of Y-82192 and QUE 93069) have similar Ti-Sm ratios and Mg#. These compositions may have resulted from mixing between HMS and FAN-rich constituents. However, another possible interpretation is that these meteorites are, in fact, FAN rocks, and the FAN and HMS rocks are more closely related than previously thought. We have attempted to further constrain these two possibilities by analyzing trace elements in single, fine-grained to microcrystalline clasts with SIMS. A major premise of these analyses is that they represent whole rock compositions of individual clasts without the influence of the meteorite matrix.

Terrestrial Weathering

It has been noted previously that desert weathering tends to alter the LREE chemistry of hot-desert meteorites,

Table 1. Bulk composition of Dho 025, Dho 081, DaG 262, DaG 400, and other lunar highland meteorites.[a]

	Dho 025	Dho 081	DaG 262	DaG 400	DaG 400	Average highland meteorites	Average mare/mixed meteorites	Average A-16 highland regolith	Average FANs	Average HMS
	(1)	(2)	(3)	(4)	(5)	(6)	(7)	(8)	(9)	(10)
SiO_2 (wt%)	43.9	44.9	n.d.[b]	43.4	n.d.	n.d.	n.d.	n.d.	44.7	45.8
TiO_2	0.30	0.15	0.22	0.23	0.18	0.27	0.57	0.38	0.09	0.30
Al_2O_3	26.1	30.5	27.5	28.6	29.2	26.3	24.8	28.4	32.9	19.0
FeO	4.98	2.93	4.40	3.52	3.78	5.24	6.60	4.18	1.71	6.45
MnO	0.08	n.d.	n.d.	0.06	0.05	0.07	n.d.	n.d.	0.03	0.09
MgO	6.53	2.82	5.21	3.80	5.14	6.10	6.80	4.53	1.62	16.6
CaO	16.1	16.8	16.5	18.7	17.4	15.4	15.8	16.4	18.6	10.7
Na_2O	0.282	0.31	0.35	0.33	0.32	0.33	0.45	0.45	0.33	0.34
K_2O	0.07	0.02	0.05	0.10	0.07	0.02	0.07	0.12	0.03	0.08
P_2O_5	0.08	n.d.	0.06	n.d.	0.11	0.02	n.d.	n.d.	0.02	0.25
H_2O	0.03	n.d.	n.d.	n.d.	n.d.	0.30	n.d.	n.d.	n.d.	n.d.
Sc (ppm)	10.2	5.40	7.85	n.d.	5.40	9.06	52.0	7.46	3.77	3.30
Cr	674	410	639	n.d.	550	699	1927	561	207	729
Co	16.5	9.80	22.0	n.d.	14.0	17.0	39.7	17.8	4.16	24.8
Ni	200	85.0	270	n.d.	113	177	87.8	212	9.56	115
Ga	3.10[c]	2.40	4.25	n.d.	n.d.	3.43	6.75	n.d.	n.d.	n.d.
Sr	2010	240	245	n.d.	190	251	159	181	159	102
Ba	130[c]	19.0	240	n.d.	140	65.5	101.5	81.9	9.59	194
Zr	62.0	n.d.	34.0	n.d.	n.d.	35.4	97.6	168	31	84
Cs	0.550	n.d.	0.120	n.d.	n.d.	0.142	0.075	0.126	0.019	0.29
La	3.60	1.43	2.44	n.d.	n.d.	2.58	7.36	6.64	0.334	7.66
Ce	8.60	3.40	7.25	n.d.	n.d.	6.60	19.1	30.9	0.838	19.9
Nd	5.20	1.90	3.25	n.d.	n.d.	3.80	13.9	18.4	0.691	12.5
Sm	1.50	0.630	1.15	n.d.	n.d.	1.17	4.00	3.10	0.131	3.10
Eu	1.30	0.700	0.730	n.d.	n.d.	0.810	1.00	1.04	0.769	1.19
Tb	0.35	0.150	0.240	n.d.	n.d.	0.243	0.880	1.12	0.036	0.663
Ho	0.44[c]	0.180	0.300	n.d.	n.d.	0.282	n.d.	n.d.	n.d.	n.d.
Yb	1.20	0.510	0.910	n.d.	n.d.	0.966	3.31	2.28	0.16	2.05
Lu	0.210	0.073	0.130	n.d.	n.d.	0.142	0.482	0.321	0.014	0.284
Hf	1.30	0.440	0.850	n.d.	n.d.	0.874	2.78	n.d.	0.126	0.804
Ta	<0.3[c]	<0.1	0.110	n.d.	n.d.	0.130	0.380	n.d.	n.d.	n.d.
Th	0.80	<10	0.430	n.d.	n.d.	0.411	0.923	1.095	0.0364	1.26
U	0.27	<300	0.210	n.d.	n.d.	0.132	0.248	0.526	n.d.	0.239
Re (ppb)	<20[c]	5.00	n.d.	n.d.	n.d.	22.5	n.d.	n.d.	n.d.	n.d.
Os	<300[c]	5.20	n.d.	n.d.	n.d.	283	n.d.	n.d.	n.d.	n.d.
Ir	7.20	0.200	12.0	n.d.	4.0	38.9	6.40	12.2	0.351	0.072
Au	3.00	0.070	4.30	n.d.	n.d.	3.27	3.10m	9.94	0.441	0.075t

[a](1) This study; (2) Warren et al. (2001); (3) Bischoff et al. (1998); (4) Semenova et al. (2000); (5) Zipfel et al. (1998); (6) Cohen et al. (2002), Palme et al. (1991), Koeberl et al. (1991), Neal et al. (1991), Spettel et al. (1995), Korotev et al. (1996), Warren et al. (2001), Bischoff et al. (1998), Semenova et al. (2000), Zipfel et al. (1998); (7) Anand et al. (2002), Jolliff et al. (1998), Lindstrom et al. (1991), Warren and Kallemeyn (1989, 1991, 1993), Koeberl (1993), Snyder et al. (1999), Fagan et al. (2002); (8) Korotev (1996); (9) and (10) Papike et al. (1988).

[b]n.d. = not determined.

[c]Elemental abundances taken from Warren et al. (2001).

particularly through alteration of olivine and pyroxenes (Crozaz and Wadhwa 2001; Crozaz et al. 2003; Floss and Crozaz 2001). However, petrogenetic information can still be extracted due to the heterogeneous nature of terrestrial weathering processes (Crozaz and Wadhwa 2001). Dho 081, DaG 262, and DaG 400 have relatively young terrestrial exposure ages (<100 kyr) (Nishiizumi et al. 2002), while Dho 025 has the oldest terrestrial exposure age of 500–600 kyr (Nishiizumi et al. 2002) of all hot-desert meteorites. Dho 025 shows a pronounced enrichment of Sr (2010 ppm), most likely due to terrestrial weathering (Table 1). Other elements that may have been affected by terrestrial weathering include Ca, Ba, and K. Dho 025, DaG 262, and DaG 400 are all elevated in Ca, Ba, and K compared to the lunar highland meteorite average, while Dho 081 is only elevated in Ca. Mineral phases that formed due to terrestrial alteration in these meteorites include barite, celestite, calcite, gypsum, and opal. Only celestite is seen frequently within Dho 025 cracks.

Although it seems logical that a longer exposure time in the desert would result in a greater amount of terrestrial alteration, studies have shown that weathering occurs most rapidly in the early part of the exposure to the terrestrial environment (Barrat et al. 1999; Bland et al. 1996; Crozaz and Wadhwa 2001). This is due to the rapid infilling of pores and fractures within the meteorite. As space within a meteorite is

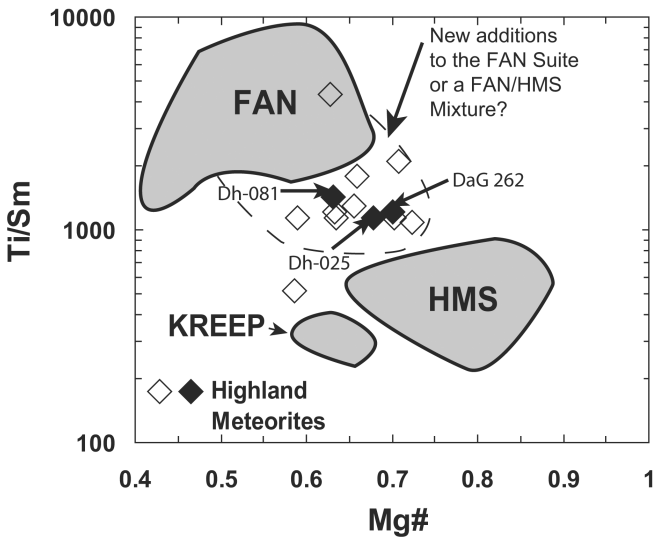

Fig. 10. Whole rock Ti/Sm versus Mg/(Mg + Fe) (Longhi and Boudreau 1979) for various lunar highlands meteorites. FAN, HMS, and KREEP compositional envelopes are shown for comparison (Taylor 1982). Dho 025, Dho 081, and DaG 262 are shown by filled diamonds (Bischoff et al. 1998; Warren et al. 2001; Zipfel et al. 1998), and lunar highlands meteorites from other studies are shown as open diamonds (Cohen et al. 2003; Koeberl et al. 1991a; Korotev et al. 1996; Neal et al. 1991; Palme et al. 1991; Semenova et al. 2000; Spettel et al. 1995).

filled with alteration material, the rate of weathering decreases with time. Thus, the high degree of terrestrial alteration observed in Dho 025 may be due to a larger volume of pore and fracture spaces in this meteorite. Indeed, a comparison of thin sections of Dho 025 and Dho 081 shows that Dho 025 has many more fractures and pore spaces than Dho 081.

TRACE ELEMENT DISTRIBUTIONS IN INDIVIDUAL CLASTS AND MINERALS

We measured minor and trace element (including REE) compositions in individual minerals (plagioclase, pyroxene and olivine) and in bulk clasts from Dho 025, Dho 081, DaG 262, and DaG 400 (Tables 2–4). With these data, we attempt to: 1) determine if any lunar meteorite clasts are pristine (retain inherited igneous chemistry) using mineral-mineral REE concentration ratios; 2) compare the mineral and clast chemistries with those of Apollo lunar samples to constrain their origins; and 3) evaluate how impact processes affected mineral compositions. A more complete account of these data can be found in Cahill (2003). Trace element concentrations typical of FAN, HMS, and high-alkali suite (HAS) minerals were compiled from the literature (Floss et al. 1998; Papike et al. 1994, 1996, 1997; Papike 1996; Shervais et al. 1997; Shervais and McGee 1998a, b, 1999; Snyder et al. Forthcoming) for comparison with Dhofar and DaG individual mineral grains. All lunar samples in these publications are considered pristine with a high level of confidence (pristinity levels of 6–8) (Warren 1993). Preliminary trace element data on Dho 025, DaG 262, and DaG 400 were presented by Cahill (2001) and Floss and Crozaz (2001).

Earlier, we noted that these meteorites have affinities to FANs (Figs. 4 and 5). However, some of the clasts plot within the FAN-HMS gap. Furthermore, whole rock data also indicate possible mixing of FAN and HMS lithologies (Fig. 10). Therefore, to evaluate this further, we analyzed single clasts, in addition to the single minerals mentioned earlier, with the ion microprobe (Table 2). We expected that analysis of fine-grained and microcrystalline clasts would eliminate the influence of matrix chemistry, the chemical mixing of several clasts, that whole rock data show and provide us with a representative clast whole rock chemistry that will allow us to trace its origin.

"Bulk" Clast Inventory

The clasts we analyzed from Dhofar and DaG highland meteorites are compared to Apollo 16, sample 67513 (2–4 mm rock fragments) (Jolliff and Haskin 1995) on a Sc versus Sm diagram (Fig. 11). Sm tracks the relative incompatible trace element (ITE) enrichment, while Sc (which is compatible in pyroxene) is an indicator of the proportion of mafic assemblage in the sample. One of two trends emerges in this type of elemental comparison (Fig. 11a). One is a ITE-depleted (Sc/Sm values >12) trend that is typical of the FAN suite (Norman and Ryder 1980), while the other ITE-rich trend is compositionally similar to impact melt breccias (Korotev 1994; Lindstrom et al. 1990). Figure 11b focuses on the ITE-depleted trend of this diagram. Low Sm and Sc abundances are indicative of plagioclase-rich mineralogies, while higher Sm and Sc concentrations are indicative of pyroxene-rich mineralogies. In general, Dhofar and DaG clasts fall along the ITE-poor trend and have characteristics similar to 67513 anorthositic rock fragments (Fig. 11b). All four meteorites are slightly depleted in Sm at a given Sc value, compared to sample 67513. This may indicate their transitional nature between FAN and HMS suites, as suggested by earlier observations. However, we cannot rule out analytical artifacts in the SIMS analyses, since ion yields are not as well-known for these bulk clast compositions as they are for single mineral analyses. Both Dho 025 and DaG 400 also have single clasts with slightly ITE and mafic mineral-rich chemistries (Sm >2.5 ppm and Sc >30 ppm).

Whole rock compositions of several other lunar highlands meteorites (MAC 88104/5, ALH A81005, Y-791197, Y-88032, and Y-82192) have elevated Sm compared to Apollo 16 sample 67513 (Jolliff et al. 1991; Jolliff and Haskin 1995; Koeberl et al. 1991a; Warren and Kallymeyn 1991). This may be because these studies used whole rock analyses (matrix + multiple clast chemistries) instead of the single clast analyses

Table 2. Bulk minor, trace, and REE concentrations (ppm) for lunar meteorite clasts.[a]

Dho 025	Clast 1	Clast 2	Clast 3	Clast 4	Clast 5	Clast 6	Clast 7	Clast 8	Clast 10
Na	2416	2023	2630	2302	2779	2038	3195	3026	2577
K	213	198	406	506	426	203	1045	493	504
Sc	4.26	7.47	11.7	11.4	30.8	3.89	20.8	17.4	31.7
Ti	195	322	752	690	2132	63	3565	1407	2253
Sr	164	141	133	1765	111	157	126	145	113
Y	1.16	3.51	3.74	4.95	12.4	1.45	25.8	9.12	11.4
Zr	3.62	15.2	13.1	15.2	22.2	1.28	154	32.9	26.7
Ba	16.0	12.7	14.3	1472	12.9	6.85	53.2	23.7	14.6
La	0.69 (2)	0.92 (5)	1.10 (7)	1.74 (8)	1.17 (4)	0.44 (4)	5.62 (19)	2.34 (9)	1.42 (7)
Ce	1.79 (5)	2.52 (10)	2.71 (14)	3.42 (13)	3.60 (12)	1.05 (7)	17.0 (4)	6.35 (23)	4.19 (15)
Pr	0.24 (1)	0.30 (2)	0.35 (2)	0.52 (3)	0.56 (3)	0.15 (1)	2.14 (10)	0.88 (5)	0.57 (4)
Nd	0.94 (2)	1.44 (5)	1.64 (7)	1.98 (9)	2.79 (9)	0.56 (2)	10.0 (3)	3.73 (12)	2.79 (10)
Sm	0.23 (2)	0.37 (3)	0.37 (4)	0.49 (3)	0.88 (4)	0.15 (1)	2.70 (15)	0.96 (7)	0.87 (6)
Eu	0.60 (2)	0.55 (2)	0.50 (3)	0.44 (9)	0.47 (2)	0.48 (3)	0.61 (4)	0.59 (3)	0.45 (3)
Gd	0.22 (2)	0.49 (4)	0.46 (6)	0.49 (6)	1.20 (7)	0.17 (2)	3.28 (23)	1.11 (9)	1.25 (9)
Tb	0.030 (4)	0.074 (7)	0.075 (7)	0.088 (9)	0.26 (2)	0.045 (4)	0.58 (5)	0.19 (2)	0.21 (2)
Dy	0.18 (1)	0.52 (3)	0.47 (3)	b.d.[b]	1.75(5)	0.20 (1)	3.63 (14)	1.35 (6)	1.54 (6)
Ho	0.036 (3)	0.11 (1)	0.12 (1)	b.d.	0.39 (2)	0.047 (6)	0.77 (4)	0.28 (2)	0.38 (3)
Er	0.13 (1)	0.34 (2)	0.34 (2)	b.d.	1.08(4)	0.14 (1)	2.29 (9)	0.85 (4)	1.11 (5)
Tm	0.013 (3)	0.040 (5)	0.065 (8)	b.d.	0.15(1)	0.012 (4)	0.32 (3)	0.11 (1)	0.15 (1)
Yb	0.078 (9)	0.28 (2)	0.36 (3)	b.d.	0.98(5)	0.12 (1)	1.92 (10)	0.74 (6)	1.02 (6)
Lu	0.014 (9)	0.048 (5)	0.074 (10)	b.d.	0.15 (1)	0.015 (3)	0.36 (4)	0.12 (1)	0.18 (2)a

Dho 081	Clast 1	Clast 2	Clast 3	Clast 4	Clast 5	Clast 6	Clast 7	Clast 8	Clast 9	Clast 10
Na	2527	2243	2039	1300	2819	2199	2558	1932	2550	2660
K	97.7	158	162	113	80.7	62.6	176	92.3	197	194
Sc	4.55	18.8	20.3	18.9	3.78	3.68	15.4	3.84	13.2	12.5
Ti	74.2	1045	1035	883	80.0	64.1	1021	113	781	770
Sr	147	126	902	131	151	140	125	149	133	136
Y	0.488	4.58	4.10	3.96	0.611	0.241	3.98	0.391	4.83	3.20
Zr	0.29	14.6	14.2	13.4	0.31	0.16	12.9	0.51	17.5	9.70
Ba	5.45	8.96	19.9	7.26	6.15	3.60	9.13	5.84	11.9	7.23
La	0.14 (1)	0.66 (3)	0.95 (5)	0.60 (4)	0.23 (1)	0.10 (1)	0.63 (3)	0.23 (2)	0.91 (4)	0.47 (3)
Ce	0.37 (2)	1.92 (7)	2.23 (9)	1.71 (9)	0.58 (3)	0.25 (1)	1.70 (7)	0.50 (4)	2.52 (8)	1.29 (7)
Pr	0.048 (3)	0.23 (2)	0.29 (2)	0.27 (2)	0.073 (5)	0.031 (3)	0.23 (1)	0.057 (7)	0.36 (1)	0.17 (1)
Nd	0.20 (1)	1.22 (4)	1.36 (5)	1.07 (4)	0.31 (1)	0.13 (1)	1.06 (3)	0.27 (1)	1.55 (4)	0.82 (3)
Sm	0.069 (6)	0.36 (3)	0.35 (3)	0.31 (3)	0.010 (9)	0.042 (6)	0.35 (2)	0.086 (13)	0.45 (2)	0.24 (2)
Eu	0.53 (2)	0.46 (2)	0.39 (2)	0.47 (3)	0.54 (2)	0.46 (2)	0.46 (2)	0.53 (2)	0.50 (2)	0.51 (2)
Gd	0.063 (6)	0.43 (3)	0.41 (4)	0.36 (4)	0.090 (9)	0.042 (6)	0.43 (3)	0.080 (12)	0.47 (4)	0.32 (3)
Tb	0.0094 (13)	0.080 (8)	0.071 (7)	0.077 (8)	0.015 (2)	0.006 (1)	0.085 (8)	0.014 (4)	0.089 (9)	0.056 (8)
Dy	0.060 (4)	0.61 (2)	0.56 (3)	0.55 (3)	0.089 (5)	0.037 (4)	0.56 (2)	0.060 (7)	0.71 (3)	0.44 (2)
Ho	0.012 (1)	0.14 (1)	0.12 (1)	0.13 (1)	0.018 (2)	0.0085 (14)	0.13 (1)	0.013 (3)	0.15 (1)	0.099 (9)
Er	0.036 (3)	0.42 (2)	0.39 (2)	0.33 (2)	0.044 (5)	0.016 (3)	0.40 (2)	0.032 (6)	0.45 (2)	0.26 (2)
Tm	0.0045 (26)	0.063 (6)	0.054 (6)	0.047 (6)	b.d.	b.d.	0.047 (5)	0.0028 (40)[c]	0.063 (7)	0.043 (6)
Yb	b.d.	0.38(2)	0.42 (3)	0.34 (2)	0.042 (5)	b.d.	0.35(2)	0.018 (7)	0.48 (2)	0.25 (2)
Lu	b.d.	0.063 (5)	b.d.	0.064 (8)	b.d.	b.d.	0.052 (5)	0.0026 (20)[c]	0.081 (6)	0.037 (8)

DaG 262	Clast 1	Clast 2	Clast 3	Clast 4	Clast 5	Clast 6	Clast 7	Clast 8	Clast 10	Clast 11
Na	2962	3226	3082	988	2896	4527	2386	3272	3810	3138
K	602	694	531	204	432	558	394	664	459	707
Sc	15	18	16	11	19	21	5.9	16	13	14
Ti	792	1043	879	420	1207	1400	48	1650	748	1523
Sr	n.r.[d]	n.r.	n.r.	n.r.	n.r.	n.r.	n.r.	n.r.	n.r.	n.r.
Y	5.2	7.6	6.3	1.4	7.3	9.9	1.3	4.7	4.5	6.2
Zr	31	35	30	6.8	35	42	3.5	87	27	52
Ba	n.r.	n.r.	n.r.	n.r.	n.r.	n.r.	n.r.	n.r.	n.r.	n.r.
La	1.08 (8)	1.96 (12)	1.37 (14)	0.40 (5)	1.51 (14)	1.84 (11)	0.33 (3)	1.62 (15)	0.96 (7)	1.50 (7)
Ce	2.82 (15)	4.88 (23	3.46 (30)	1.06 (9)	3.23 (29)	5.74 (30)	0.64 (4)	3.02 (26)	1.96 (12)	3.91 (16)
Pr	0.46 (3)	0.66 (5)	0.32 (4)	0.085 (16)	0.48 (5)	0.73 (5)	0.10 (1)	0.45 (4)	0.29 (3)	0.59 (4)

Table 2. Bulk minor, trace, and REE concentrations (ppm) for lunar meteorite clasts.[a] *Continued.*

DaG 262	Clast 1	Clast 2	Clast 3	Clast 4	Clast 5	Clast 6	Clast 7	Clast 8	Clast 10	Clast 11
Nd	1.50 (6)	2.70 (11)	1.78 (13)	0.51 (4)	1.98 (13)	3.35 (13)	0.36 (2)	1.87 (13)	1.11 (7)	2.32 (9)
Sm	0.47 (5)	0.60 (6)	0.49 (7)	0.14 (4)	0.72 (8)	0.85 (8)	0.10 (2)	0.44 (8)	0.26 (5)	0.62 (6)
Eu	0.45 (6)	0.62 (9)	0.49 (11)	0.13 (5)	0.40 (14)	0.39 (7)	0.35 (7)	0.20 (19)	0.37 (6)	0.66 (7)
Gd	0.47 (6)	0.92 (11)	0.60 (11)	0.20 (4)	0.57 (13)	1.11 (13)	0.12 (2)	0.47 (11)	0.35 (6)	0.58 (8)
Tb	0.11 (1)	0.14 (1)	0.11 (3)	0.03 (8)	0.13 (3)	0.19 (3)	0.024 (5)	0.091 (20)	0.068 (12)	0.10 (2)
Dy	0.66 (4)	1.11 (5)	0.77 (8)	0.16 (2)	0.93 (9)	1.41 (7)	0.18 (2)	0.67 (6)	0.58 (5)	0.79 (5)
Ho	0.15 (2)	0.28 (2)	0.24 (4)	0.042 (10)	0.24 (3)	0.27 (2)	0.068 (8)	0.14 (2)	0.13 (1)	0.18 (2)
Er	0.40 (3)	0.77 (5)	0.57 (6)	0.11 (2)	0.75 (6)	0.89 (6)	0.12 (2)	0.50 (5)	0.46 (4)	0.50 (3)
Tm	0.078 (10)	0.080 (16)	0.071 (20)	0.035 (10)	0.10 (2)	0.14 (1)	0.011 (6)	0.058 (20)	0.067 (14)	0.046 (9)
Yb	0.45 (6)	0.64 (6)	0.53 (10)	0.22 (4)	0.56 (9)	0.86 (8)	0.11 (2)	0.35 (9)	0.50 (8)	0.41 (5)
Lu	0.060 (12)	0.11 (1)	0.061 (17)	0.034 (12)	0.11 (2)	0.13 (2)	0.017 (6)	0.055 (18)	0.095 (17)	0.050 (11)
DaG 400	Clast 1	Clast 2	Clast 3	Clast 4	Clast 5	Clast 6	Clast 7			
Na	2232	3285	1753	2517	643	3701	2745			
K	926	895	824	497	368	1669	1166			
Sc	22	19	8.7	20	10	34	5.6			
Ti	1293	1273	303	1342	941	4659	924			
Sr	n.r.	n.r.	n.r.	n.r.	n.r.	n.r.	n.r.			
Y	16	7.8	0.95	9.0	2.6	33	2.8			
Zr	46	28	2.84	41.7	9.5	146	4.2			
Ba	n.r.	n.r.	n.r.	n.r.	n.r.	n.r.	n.r.			
La	1.18 (1)	1.24 (13)	0.25 (5)	1.75 (12)	0.29 (3)	6.30 (39)	0.63 (6)			
Ce	4.00 (27)	3.35 (26)	0.62 (5)	4.97 (31)	0.49 (4)	15.4 (69)	1.74 (15)			
Pr	0.70 (7)	0.48 (5)	0.09 (1)	0.72 (6)	0.069 (9)	2.08 (14)	0.16 (2)			
Nd	2.55 (16)	2.31 (13)	0.41 (3)	2.54 (13)	0.31 (2)	9.45 (38)	0.74 (5)			
Sm	1.12 (14)	0.61 (10)	0.11 (2)	0.91 (11)	0.10 (2)	2.50 (2)	0.21 (4)			
Eu	0.35 (5)	0.53 (6)	0.34 (3)	0.41 (4)	0.046 (67)[c]	0.41 (8)	0.48 (4)			
Gd	1.39 (17)	0.65 (12)	0.077 (23)	0.95 (13)	0.12 (2)	2.50 (38)	0.24 (5)			
Tb	0.36 (5)	0.13 (2)	0.017 (5)	0.22 (3)	0.036 (6)	0.62 (7)	0.056 (10)			
Dy	2.23 (15)	0.98 (7)	0.11 (2)	1.28 (8)	0.29 (2)	4.12 (23)	0.43 (4)			
Ho	0.44 (5)	0.21 (2)	0.035 (6)	0.22 (3)	0.075 (9)	0.83 (11)	0.076 (14)			
Er	1.46 (10)	0.78 (7)	0.092 (13)	0.74 (5)	0.29 (2)	2.74 (13)	0.20 (3)			
Tm	0.22 (3)	0.066 (12)	b.d.	0.089 (2)	0.038 (6)	0.32 (4)	0.023 (9)			
Yb	1.16 (16)	0.55 (7)	b.d.	0.85 (8)	0.28 (3)	2.30 (34)	b.d.			
Lu	0.14 (3)	0.10 (2)	0.011 (5)	0.12 (2)	0.036 (7)	0.48 (8)	0.020 (8)			

[a]Errors are 1σ due to counting statistics.
[b]b.d. = below detection.
[c]Note the larger than normal errors.
[d]n.r. = values not reported due to probable terrestrial contamination. See Floss and Crozaz (2001).

of this study and that of Jolliff and Haskin (1995). Dhofar and DaG clast analyses clearly show stronger affinities to FAN than previously seen in whole rock analyses (Bischoff et al. 1998; Semenova et al. 2000; Zipfel et al. 1998).

Compositional Mixing Model

A closer examination of the REE concentrations of Dhofar and DaG clasts compared to FAN and HMS rocks suggests the possibility that Dhofar and DaG chemistries were subjected to a degree of mixing. Mixing of average HMS components and average FAN composition (Papike 1998) and comparison with the clast data show that clasts from all four meteorites contain an appreciable HMS component. Most Dhofar and DaG clasts show ≤12% HMS component, but one DaG 400 clast contains 62% of an HMS component and one Dho 025 clast contains 71% of an HMS component.

Plagioclase Inventory

The REE patterns for individual plagioclase grains from Dho 025, Dho 081, DaG 262, and DaG 400 are shown in Fig. 12. All plagioclase analyses have REE abundances similar to those seen in FAN rocks. However, some Dho 025 clasts have plagioclases that are enriched in heavy rare earth elements (HREE) compared to typical pristine FAN plagioclase (Fig. 12a). In addition, light rare earth elements (LREE) in Dho 025 plagioclase tend to be enriched relative to plagioclase from Dho 081, DaG 262, and DaG 400. Despite the HREE enrichments in many Dho 025 plagioclase grains, five grains show REE trends typical of pristine FAN lithologies (clasts AA, AI, 108b, BA, and BB; Fig. 12a). All Dho 081 plagioclases have lower REE abundances than those in the other meteorites analyzed, with patterns that fall toward the lower end of the range observed for FANs (Fig. 12b). DaG

Table 3. Major, minor, trace, and REE concentrations (ppm) of Dho 025 lunar highlands plagioclase.[a]

	Dho 025											
	AA	AB	AF	AI	108b	AE	AG	BA	BB	BD	BH	BL
Na	2420	1504	2363	1612	3361	4246	2961	2141	1746	2461	2193	3471
Mg	666	1410	986	732	727	721	714	619	769	816	1311	1226
K	68	111	179	117	152	397	242	98	85	204	242	194
Ca	126789	129617	126143	125922	124663	121047	122414	126255	127081	130594	128096	125814
Sc	3.5	4.4	4.4	3.5	3.4	3.1	4.4	3.4	3.8	4.1	4.2	3.9
Ti	87	226	235	56	125	204	193	94	57	434	265	218
Fe	1437	2428	1978	1291	1054	1526	1501	1492	1512	1997	2528	2072
Sr	114	110	120	107	111	138	110	107	103	109	109	114
Y	0.5	3.6	3.6	0.7	0.6	2.2	1.8	0.8	0.7	3.7	4.3	3.7
Zr	0.3	6.7	7.3	0.3	0.2	3.0	10.9	0.6	1.0	14.8	11.1	8.5
Ba	6.0	5.8	12.5	5.0	8.7	27.0	16.6	7.0	2.5	13.7	10.9	7.4
La	0.68 (8)	0.77 (6)	1.52 (7)	0.49(4)	1.06 (8)	2.31 (16)	2.14 (12)	0.82 (8)	0.31 (4)	1.76 (8)	1.39 (9)	0.84 (6)
Ce	1.69 (18)	2.32 (13)	4.13 (15)	1.15 (7)	2.35 (18)	5.96 (35)	5.97 (30)	1.91 (11)	0.82 (8)	4.18 (20)	3.75 (24)	2.89 (15)
Pr	0.21 (3)	0.32 (2)	0.54 (2)	0.16 (2)	0.29 (3)	0.68 (4)	0.70 (5)	0.31 (3)	0.10 (2)	0.56 (4)	0.45 (4)	0.37 (2)
Nd	0.85 (7)	1.38 (5)	2.18 (6)	0.62 (4)	1.11 (7)	2.33 (13)	2.97 (11)	1.00 (6)	0.42 (4)	2.25 (8)	2.11 (11)	1.60 (7)
Sm	0.15 (4)	0.38 (6)	0.57 (5)	0.20 (3)	0.20 (4)	0.53 (7)	0.52 (6)	0.17 (4)	0.10 (4)	0.52 (5)	0.63 (9)	0.50 (5)
Eu	0.84 (5)	0.77 (4)	0.89 (4)	0.85 (4)	0.72 (5)	1.09 (7)	0.87 (5)	0.74 (5)	0.70 (4)	0.74 (4)	0.77 (5)	0.85 (3)
Gd	0.11 (5)	0.49 (5)	0.61 (7)	0.13 (3)	0.20 (5)	0.58 (10)	0.37 (8)	0.14 (5)	0.11 (4)	0.55 (7)	0.54 (10)	0.63 (6)
Tb	0.021 (9)	0.070 (11)	0.10 (1)	0.015 (6)	0.017 (9)	0.076 (19)	0.057 (13)	0.024 (1)	0.029 (10)	0.10 (1)	0.13 (2)	0.10 (1)
Dy	0.092 (20)	0.49 (3)	0.66 (3)	0.13 (2)	0.087 (20)	0.43 (4)	0.36 (3)	0.095 (21)	0.13 (3)	0.66 (4)	0.90 (7)	0.69 (4)
Ho	0.01 9 (9)	0.11 (1)	0.11 (1)	0.023 (6)	0.028 (9)	0.063 (13)	0.086 (11)	0.018 (7)	0.013 (7)	0.15 (2)	0.16 (2)	0.14 (1)
Er	0.052 (18)	0.29 (3)	0.36 (2)	0.035 (13	0.051 (18)	0.25 (4)	0.18 (2)	0.081 (20)	0.056 (20)	0.33 (3)	0.46 (5)	0.36 (3)
Tm	0.0055 (58)[b]	0.050 (11)	0.059 (9)	b.d.[c]	b.d.	0.030 (15)	b.d.	b.d.	b.d.	0.063 (11)	0.042 (17)	0.04 (1)
Yb	0.031 (24)	0.29 (4)	0.31 (3)	0.046 (19)	0.040 (24)	0.17 (4)	0.11 (3)	0.092 (30)	b.d.	0.34 (3)	0.39 (7)	0.30 (4)
Lu	b.d.	0.024 (9)	0.051 (8)	b.d.	b.d.	b.d.	b.d.	b.d.	0.0055 (80)[b]	0.05 (1)	b.d.	0.042 (11)
	Dho 081						DaG 262			DaG 400		
	AE	C	F	H	L	V	1	2	3	1	2	3
Na	2293	2471	2428	2240	2446	1996	2438	2998	3098	2713	3969	3418
Mg	472	667	418	886	1006	573	1162	3725	3425	925	446	1098
K	74	66	128	58	86	53	143	288	263	515	301	494
Ca	123739	125963	123937	128879	124359	124199	125124	126984	107470	127627	131551	129481
Sc	3.9	3.6	2.9	3.5	3.2	4.2	3.4	4.4	3.2	3.0	3.4	4.0
Ti	36	82	28	32	56	21	80	68	90	118	62	171
Fe	1328	1294	1511	1615	1995	1511	1539	1667	1712	1092	1878	1224
Sr	104	115	111	103	100	104	n.r.[d]	n.r.	n.r.	n.r.	n.r.	n.r.
Y	0.4	0.7	0.4	0.2	0.3	0.2	0.6	0.5	0.5	0.9	0.8	0.7
Zr	0.2	0.3	0.2	0.7	0.2	0.1	1.0	2.1	2.9	0.4	0.2	0.3
Ba	4.1	4.4	8.5	3.1	3.8	2.4	n.r.	n.r.	n.r.	n.r.	n.r.	n.r.

Table 3. Major, minor, trace, and REE concentrations (ppm) of Dho 025 lunar highlands plagioclase.[a] *Continued.*

	Dho 081						DaG 262			DaG 400		
	AE	C	F	H	L	V	1	2	3	1	2	3
La	0.23 (3)	0.32 (3)	0.19 (2)	0.13 (1)	0.13 (2)	0.094 (15)	0.76 (4)	0.38 (3)	0.29 (3)	0.80 (5)	0.51 (4)	0.95 (5)
Ce	0.63 (7)	0.81 (6)	0.44 (4)	0.30 (3)	0.35 (4)	0.19 (3)	2.04 (9)	1.04 (7)	0.67 (5)	1.88 (11)	1.33 (7)	2.26 (11)
Pr	0.10 (1)	0.13 (1)	0.054 (12)	0.034 (7)	0.05 (1)	0.043 (9)	0.25 (2)	0.12 (1)	0.10 (1)	0.26 (2)	0.17 (1)	0.30 (2)
Nd	0.41 (4)	0.38 (3)	0.26 (3)	0.17 (2)	0.19 (3)	0.094 (18)	0.93 (5)	0.39 (3)	0.39 (3)	1.02 (5)	0.66 (3)	1.07 (4)
Sm	0.076 (31)	0.10 (3)	b.d.	b.d.	b.d.	b.d.	0.17 (3)	0.097 (24)	0.11 (3)	0.27 (4)	0.17 (2)	0.27 (3)
Eu	0.71 (5)	0.72 (3)	0.79 (5)	0.60 (3)	0.61 (4)	0.60 (4)	0.67 (3)	0.81 (8)	0.44 (6)	0.68 (4)	0.88 (4)	0.75 (3)
Gd	0.074 (27)	0.14 (3)	0.034 (26)	0.038 (16)	0.032 (19)	b.d.	0.16 (3)	0.098 (23)	0.081 (23)	0.23 (4)	0.16 (3)	0.17 (3)
Tb	0.007 (6)	0.016 (7)	0.0092 (75)	0.0073 (43)	b.d.	0.0025 (37)[b]	0.013 (6)	0.0062 (44)	0.012 (5)	0.025 (8)	0.025 (6)	0.026 (6)
Dy	0.034 (14)	0.12 (2)	0.035 (18)	0.039 (11)	0.020 (10)	b.d.	0.11 (2)	0.093 (15)	0.077 (13)	0.14 (2)	0.13 (1)	0.13 (1)
Ho	0.0059 (50)[b]	0.027 (8)	b.d.	0.016 (5)	b.d.	0.0023 (34)[b]	0.017 (5)	0.051 (8)	0.036 (7)	0.033 (7)	0.035 (6)	0.033 (5)
Er	0.012 (13)[b]	0.037 (14)	0.0082 (142)[b]	0.028 (11)	b.d.	0.0039 (77)[b]	0.050 (12)	0.068 (14)	0.049 (12)	0.055 (15)	0.043 (10)	0.051 (11)
Tm	b.d.	b.d.	b.d.	b.d.	b.d.	b.d.	b.d.	b.d.	b.d.	0.011 (8)	b.d.	0.0051 (57)[c]
Y	b.d.	0.021 (17)[b]	b.d.	b.d.	b.d.	b.d.	0.056 (19)	0.035 (21)	0.038 (19)	0.036 (19)	0.055 (19)	0.043 (15)
Lu	b.d.	0.0014 (55)[b]	b.d.	b.d.	b.d.	b.d.	b.d.	b.d.	b.d.	b.d.	0.0051 (39)	b.d.

[a]Errors are 1σ due to counting statistics.
[b]Note the larger than normal errors.
[c]b.d. = below detection.
[d]n.r. = values not reported due to probable terrestrial contamination. See Floss and Crozaz (2001).

Table 4. Major, minor, trace, and REE concentrations (ppm) of Dho 025, Dho 081, DaG 262, and DaG 400 pyroxene and olivine.[a]

	Dho 025								Dho 081	DaG 262		DaG 400
	108b opx	BM opx	ACB pig	108b aug	108b aug	BA aug	BH aug	BL aug	F opx	1 aug	2 opx	1 ol
Na	144	120	339	692	558	487	518	583	116	291	183	104
Mg	158268	165688	144925	98878	104638	103798	109237	162851	154448	70780	112336	223297
K	132	78	206	103	103	79	123	365	53	163	185	75
Ca	12201	9392	24729	114243	117264	107434	107773	69010	12010	88824	13338	1089
Sc	24	25	29	52	56	60	75	55	26	95	30	8
Ti	3247	3439	2691	6229	6474	4632	5477	5164	3478	3001	2687	159
Fe	57316	54422	81324	35572	38760	50516	42399	163533	93678	305743	192382	220049
Sr	4.4	6.4	8.6	8.2	9.6	8.9	37	58	1.2	n.r.[b]	n.r.	n.r.
Y	7.5	9.2	10	41	39	33	36	32	7.5	57	5.2	0.19
Zr	26	27	27	180	155	120	126	74	21	107	6.0	0.25
Ba	0.63	0.35	2.2	3.1	1.2	1.7	33	1.7	0.14	n.r.	n.r.	n.r.
La	0.14 (1)*	0.27 (4)	0.37 (5)	1.73 (13)	1.05 (9)	0.86 (9)	0.92 (9)	0.98 (9)	0.028 (6)	0.71 (9)	b.d.[c]	b.d.
Ce	0.51 (4)	0.86 (11)	1.39 (14)	7.19 (40)	5.43 (32)	4.37 (35)	4.55 (29)	3.99 (29)	0.093 (14)	3.47 (33)	b.d.	b.d.
Pr	0.077 (12)	0.089 (21)	0.19 (2)	1.47 (12)	1.32 (10)	0.90 (8)	1.00 (8)	0.83 (7)	0.026 (6)	0.89 (9)	b.d.	b.d.

Table 4. Major, minor, trace, and REE concentrations (ppm) of Dho 025, Dho 081, DaG 262, and DaG 400 pyroxene and olivine.[a] *Continued.*

	Dho 025											
	108b	BM	ACB	108b	108b	BA	BH	BL	F	1	2	1
	opx	opx	pig	aug	aug	aug	agu	aug	opx	aug	opx	ol
Nd	0.42 (3)	0.51 (6)	1.12 (8)	8.14 (36)	7.52 (35)	5.16 (31)	5.34 (23)	4.67 (23)	0.21 (2)	5.79 (31)	b.d.	b.d.
Sm	0.27 (4)	0.19 (6)	0.43 (6)	3.74 (23)	3.65 (33)	2.25 (25)	2.90 (25)	2.42 (16)	0.19 (3)	2.64 (29)	b.d.	b.d.
Eu	0.0068 (45)	0.0032 (69)[d]	0.0024 (89)[d]	0.049 (21)	0.056 (24)	0.0003 (215)[d]	0.063 (30)	0.082 (15)	0.008 (4)	0.030 (58)[d]	b.d.	b.d.
Gd	0.51 (5)	0.44 (9)	0.83 (11)	4.69 (47)	4.98 (44)	3.60 (47)	0.34 (35)	3.21 (38)	0.32 (6)	6.26 (58)	b.d.	b.d.
Tb	0.14 (1)	0.13 (2)	0.19 (2)	0.97 (8)	1.21 (11)	0.70 (12)	0.91 (7)	0.61 (7)	0.086 (12)	1.21 (12)	0.056 (7)	b.d.
Dy	1.04 (5)	1.10 (9)	1.61 (10)	6.57 (31)	6.66 (32)	4.57 (35)	0.05 (25)	5.45 (28)	0.93 (5)	7.59 (44)	0.60 (3)	b.d.
Ho	0.25 (2)	0.33 (4)	0.33 (3)	1.52 (12)	1.44 (9)	0.96 (12)	1.17 (9)	1.15 (11)	0.20 (2)	1.84 (16)	0.18 (2)	0.0086 (24)
Er	0.97 (5)	1.19 (8)	1.24 (7)	4.03 (22)	3.83 (20)	3.18 (24)	3.80 (16)	3.53 (19)	0.82 (5)	5.96 (34)	0.72 (3)	0.029 (5)
Tm	0.13 (1)	0.18 (2)	0.24 (3)	0.47 (5)	0.46 (5)	0.37 (5)	0.45 (4)	0.47 (4)	0.12 (2)	0.96 (10)	0.12 (1)	0.0053 (21)
Yb	1.05 (6)	1.38 (14)	1.16 (11)	2.71 (25)	2.98 (23)	2.23 (27)	2.63 (22)	2.49 (25)	1.01 (9)	7.06 (64)	0.80 (7)	0.082 (14)
Lu	0.19 (2)	0.25 (3)	0.23 (3)	0.41 (6)	0.44 (7)	0.32 (8)	0.37 (5)	0.41 (6)	0.19 (3)	1.10 (16)	0.19 (2)	0.0082 (30)

[a]Errors are 1σ due to counting statistics.
[b]n.r. = values not reported due to probable terrestrial contamination. See Floss and Crozaz (2001).
[c]b.d. = below detection.
[d]Note the larger than normal errors.

262 and DaG 400 also have plagioclase REE concentrations falling within the typical FAN suite.

Concentrations of Ce, K, and Ba in plagioclase grains are similar to those of other FAN suite rocks (Fig. 13). However, Fe and Mg abundances are elevated, while Sr is depleted, although still similar to FAN plagioclases. This suggests that the terrestrial Sr influx in Dho 025, interpreted from whole rock data, is dominated by surficial additions of terrestrial Sr-bearing minerals and that exchange with Dho 025 plagioclase was limited. Furthermore, Sr and Ba concentrations show slight positive trends with increasing La abundance (Fig. 14), similar to trends seen in other highlands rocks (Floss et al. 1998; Snyder et al. 2003, personal communication). This suggests that Sr may behave incompatibly in lunar plagioclases despite the fact that its partition coefficient ($K_{D\,Sr}$) is 1.61 (Phinney and Morrison 1990).

Pyroxene Inventory

REEs in low-Ca pyroxenes from Dho 025, Dho 081, and DaG 262 have concentrations similar to those from typical FAN and HMS rocks (Figs. 15a and 15b). Dho 025 and Dho 081 low-Ca pyroxenes have Ce and Zr abundances similar to those observed in FAN rocks but appear to be slightly depleted in both Sc and Y (Fig. 16). However, Sc and Y concentrations fall along the trends observed for FANs, while HMS and HAS rocks define steeper slopes, particularly for Y (Fig. 16).

High-Ca pyroxenes in Dho 025 and DaG 262 have REE abundances similar to those of FAN high-Ca pyroxenes (Fig. 15c). One Dho 025 analysis has a much deeper negative Eu anomaly (0.01 × CI) than the rest, although it also falls within the FAN compositional range, within 1σ errors. Cerium and Zr are positively correlated, similar to the trend seen in FANs (Fig. 16). Yttrium concentrations are also similar to those in the FANs, but Sc is low in Dho 025 compared to DaG 262 and other FAN pyroxenes.

Olivine Inventory

A few SIMS trace element analyses have been reported for olivines from FAN lithologies (Floss et al. 1998). Generally, the low abundances of LREE in olivine do not allow their quantitative determination with this technique. Furthermore, the small size of olivine grains in the meteorites that we studied did not allow SIMS measurements in any troctolitic-anorthosite clasts. However, one olivine grain was successfully analyzed in DaG 400 (Fig. 15d). This grain has low HREE abundances (≤0.5 × CI) and falls at the low end of the range observed for FAN olivines.

Plagioclase-Pyroxene REE Ratios

It is possible to evaluate whether a rock or clast represents an equilibrium assemblage by comparing

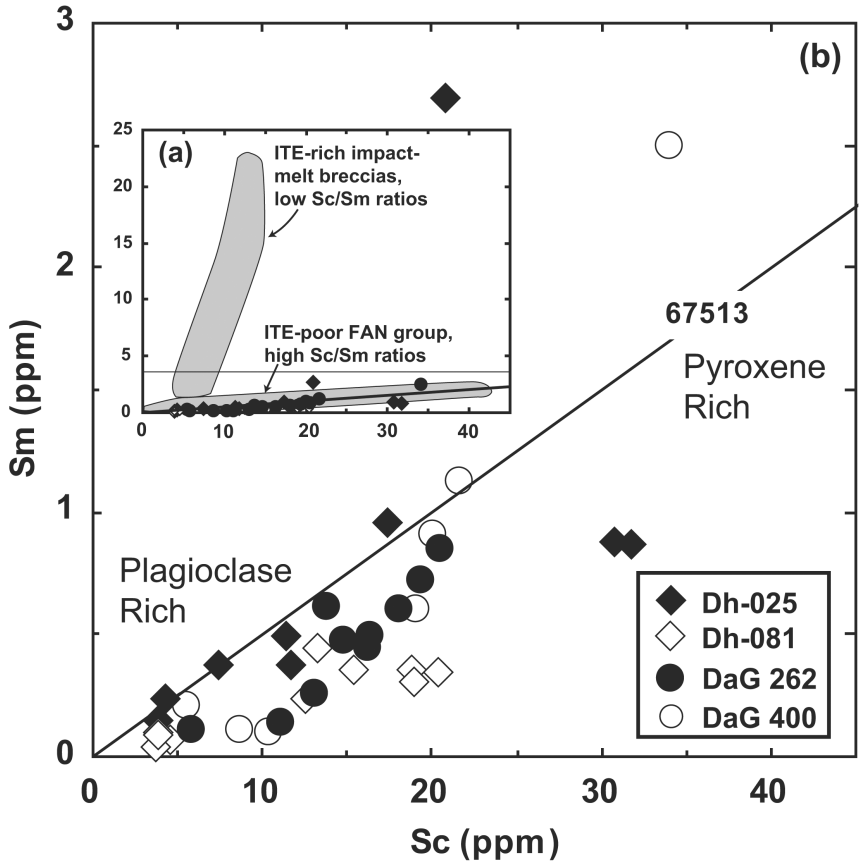

Fig. 11. Apollo 16 samples show two compositional trends in terms of Sc and Sm as illustrated in (a). Impact melt breccias are incompatible trace element (ITE)-rich, while ferroan anorthosites (FAN) are ITE-poor (Jolliff and Haskin 1995; Korotev 1994); b) enlargement of ITE-poor portion of diagram (a). Dho 025, Dho 081, DaG 262, and DaG 400 have Sm and Sc concentrations similar to ITE-poor and plagioclase-rich lithologies.

plagioclase-pyroxene REE concentration ratios (i.e., $C^{Pl}_{REE}/C^{Px}_{REE}$) with experimentally determined mineral-melt partition coefficient ratios for plagioclase and pyroxene (i.e., $K_D{}^{Pl}_{REE}/K_D{}^{Px}_{REE}$). It should be noted that all the polymineralic clasts we analyzed have non-relict textures.

In Fig. 17, the concentration ratios of several impact-melt clasts are compared with the ratios expected from experimentally determined distribution coefficients. If a rock, or clast, preserves the chemical signature inherited from its parental melt, then these ratios should be identical. The assumption that the chosen K_D values are valid is inherent here.

Distribution coefficients were selected from studies by McKay et al. (1986, 1991) and Weill and McKay (1975). Mineral-melt ratio errors are 1σ, based on a partition coefficient uncertainty of 20% (McKay 1989). Since pyroxene distribution coefficients are sensitive to their Ca contents, each clast's pyroxene K_D value was calculated individually (McKay et al. 1986). We used caution with orthopyroxene, since K_D values were determined at a time when the difficulties in measuring low concentrations of the REE with electron microprobe were not fully appreciated (McKay 1989; Weill and McKay 1975). Out of the five clasts evaluated, only two (108b and BA) show plagioclase-pyroxene ratios concordant with those of experimentally determined plagioclase-pyroxene ratios (Fig. 17). Clast 108b ratios were corroborated using three sets of coexisting minerals within this clast. Clast BA also has a concordant plagioclase-pyroxene ratio, although the error associated with Eu is large. All other clasts have discordant plagioclase-pyroxene ratios indicating that the coexisting minerals do not represent magmatic equilibrium conditions.

DISCUSSION

In this study, we analyzed several clasts for their trace element concentrations in an attempt to find if these lunar samples contain equilibrium mineral assemblages. We approached this task by evaluating plagioclase-pyroxene REE ratios, as described in the previous section. Clasts with concordant REE ratio patterns are likely samples that contain unmodified chemical information from a parental melt and may be considered pristine lithologies. Of the clasts analyzed, the mineral REE ratios show that the minerals in two Dho 025 clasts (108b and BA) have retained equilibrium with a parent

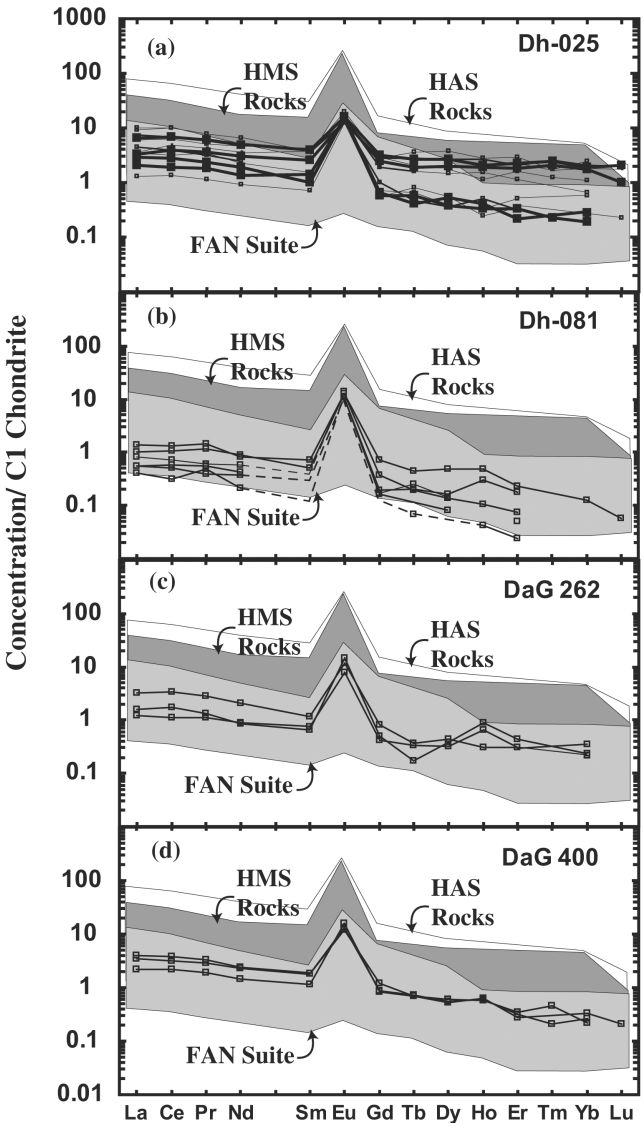

Fig. 12. C1-chondrite normalized REE patterns for plagioclase grains from lunar meteorites Dho 025 (a), Dho 081 (b), DaG 262 (c), and DaG 400 (d). The normalization values are from Anders and Grevesse (1989). These patterns are compared to pristine plagioclase grains from FAN, HMS, and (high-alkali suite) HAS rocks (Floss et al. 1998; Papike et al. 1996, 1997; Shervais et al. 1997; Shervais and McGee 1998a, b, 1999; Snyder et al. 2004). The Dho 025 patterns with bold lines and symbols represent clasts that were designated as texturally "pristine" in this study.

melt (Fig. 17). However, the other three clasts show discordant REE ratio profiles when compared to experimentally determined REE ratios. Despite not representing equilibrium assemblages, clasts with discordant REE ratio profiles can still provide insight about the processes that modified them. Discordant REE ratio profiles can result from several processes, including: 1) use of incorrect distribution coefficients; 2) subsolidus re-equilibration; and 3) impact processes, all of which are evaluated below.

Distribution Coefficients

Of foremost concern when determining REE ratios is the use of appropriate experimental distribution coefficients. Plagioclase melt partition coefficients for the REEs have been studied specifically for lunar conditions (McKay 1982; Phinney and Morrison 1990; Weill and McKay 1975), and values determined experimentally and by direct measurement are in good agreement (Phinney and Morrison 1990). Thus, distribution coefficients for plagioclase REEs are unlikely to be a large source of error here.

In contrast, the behavior of REEs in pyroxene has not been rigorously evaluated for lunar conditions. Pyroxene distribution coefficients have been determined, but they were determined for a shergottite composition and oxidation state (McKay et al. 1986). Despite this, preliminary work on clinopyroxene partitioning under lunar conditions does not indicate substantial differences in distribution coefficients compared to the more oxidizing conditions appropriate for shergottite crystallization (McKay et al. 1991). Thus, oxygen fugacity does not appear to have a large effect on the K_D values for trivalent REEs in pyroxene (James et al. 2002). Partition coefficient values used for orthopyroxene have also been noted to be a topic of concern, as mentioned earlier (Floss et al. 1998; McKay 1989); however, no inherent problems with these distribution coefficients were evident in this study.

Subsolidus Re-Equilibration

Subsolidus re-equilibration can also cause discordant mineral REE ratios (Floss et al. 1998; James et al. 2002; Papike 1996; Treiman 1996). This process generally involves material that has undergone extensive recrystallization and prolonged thermal metamorphism (Floss et al. 1998). Re-equilibration can occur within zoned minerals or between coexisting minerals. Homogenization of zoned minerals will cause higher average REE concentrations than those of the original mineral cores (Floss et al. 1998). Plagioclase-pyroxene REE ratios will have lower and less steep patterns than experimental REE ratio patterns (Hsu and Crozaz 1996, 1997).

Recent ion microprobe studies have also demonstrated that both the HREEs and LREEs may be redistributed between co-existing pyroxene and plagioclase in a manner dependent upon their crystal chemistries (Papike 1996; Papike et al. 1996). During co-existing mineral re-equilibration, plagioclase is depleted in HREE, and pyroxene is depleted in LREE. The resulting REE ratio pattern would have a steeper negative trend than would a pattern reflecting experimentally determined distribution coefficients.

Problems are also prevalent when considering augite and orthopyroxene formed by inversion of pigeonite (James et al. 2002). Upon inversion, extensive internal redistribution of major, minor, and trace elements are required for the necessary structural changes to occur. As inversion of

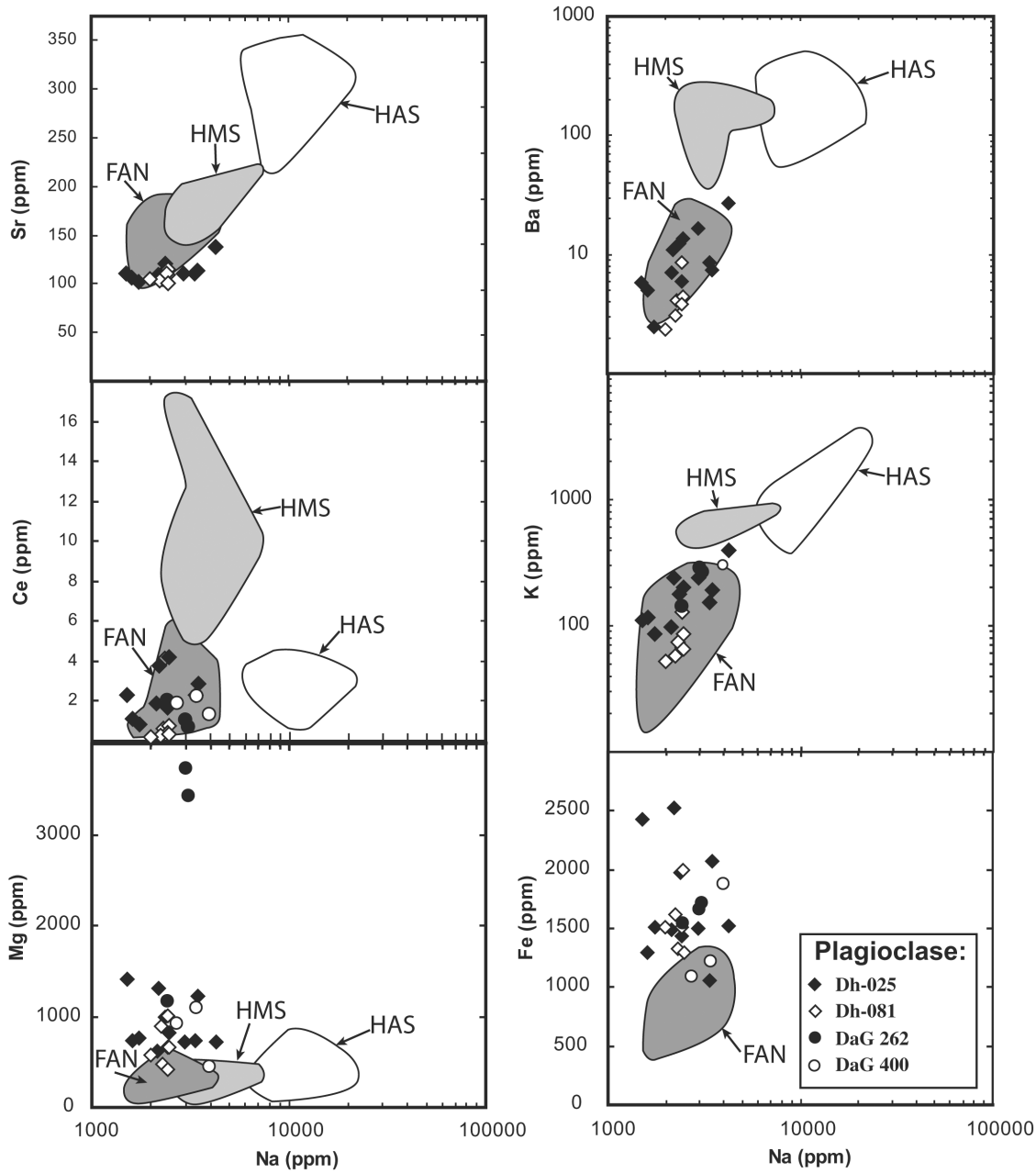

Fig. 13. Minor and trace element data for plagioclase grains from lunar highlands meteorites Dho 025, Dho 081, DaG 262, and DaG 400 compared to that of pristine FAN, HMS, and (high-alkali suite) HAS plagioclase (Floss et al. 1998; Snyder et al. 2004).

pigeonite and subsequent subsolidus re-equilibration take place, REEs move from orthopyroxene into augite, with HREEs migrating with a greater mobility than LREEs (James et al. 2002). Orthopyroxene-augite REE ratios develop lower and steeper positive trends. Furthermore, migration of LREEs from orthopyroxene to augite will result in plagioclase-augite REE ratio patterns with steeper negative trends.

The REE ratio patterns for discordant clasts tend to be flatter than the expected K_D ratio patterns (Fig. 17). This may indicate that these minerals were previously zoned and have homogenized, although homogenization usually entails lower overall patters in addition to flatter slopes. Thus, subsolidus re-equilibration may have been one, but not the only, influence on their REE ratio patterns.

Impact Processes

Impact-induced mixing, as discussed for the whole rock and clast analyses of these meteorites, may have influenced some of the mineral analyses. When impact processes occur, some amount of material may be vaporized, and a larger amount of material will be melted and/or partially melted.

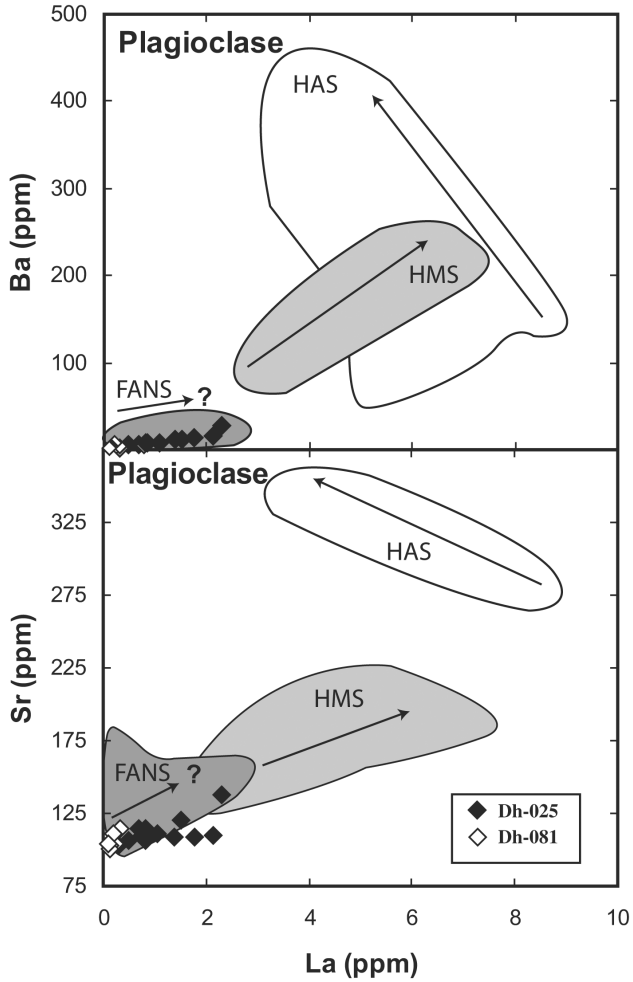

Fig. 14. Plagioclase Ba, Sr, and La systematics for lunar meteorites Dho 025 and Dho 081 compared to FAN, HMS, and high-alkali suite (HAS) data (Floss et al. 1998; Papike et al. 1997; Snyder et al. 2004).

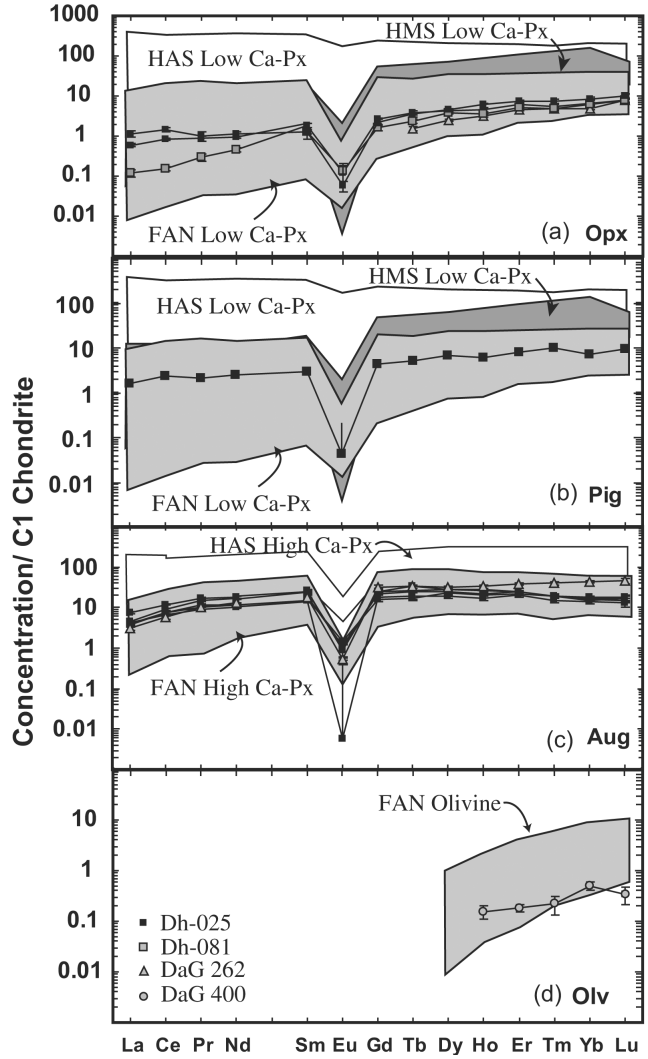

Fig. 15. C1-chondrite normalized REE patterns for pyroxenes and olivine grains. Normalization values are from Anders and Grevesse (1989). Orthopyroxene (a) and pigeonite (b) REEs are compared to pristine low-Ca pyroxene data of FAN, HMS, and high-alkali suite (HAS) rocks (Floss et al. 1998; Papike et al. 1994, 1996; Papike 1996; Shervais et al. 1997; Shervais and McGee 1998a, b, 1999; Snyder et al. 2004). High-Ca pyroxene (c) and olivine (d) analyses are compared to pristine analyses from FAN rocks (Floss et al. 1998).

Certain volatile minor elements, such as Na and K, are likely to be affected. However, it is also important to consider how the REEs would react to such an event.

As shown in Fig. 13, Fe and Mg concentrations are elevated in the lunar meteorite plagioclase grains compared to FAN, HMS, and HAS plagioclase. This suggests that impact metamorphism has affected these clasts. However, Fe concentrations do not surpass the upper limit for FeO in primary igneous plagioclases from Apollo 14 highlands rocks (1 wt% FeO) (Stöffler and Knöll 1977). Furthermore, Na and K concentrations in clast plagioclases are similar to FAN lithologies (Fig. 13) and do not suggest volatilization. In addition, optical analyses of feldspar crystals do not exhibit isotropic characteristics typical of maskelynite.

However, impact modification does appear to have affected the REE concentrations of some Dho 025 plagioclase grains (Fig. 12a) in which the HREE are disproportionately enriched. The source of these REE enrichments could be exchange with a surrounding impact melt or a coexisting pyroxene. During normal igneous processes, pyroxene has a lower melting point than olivine and anorthite, while the dynamics of impact-induced melting are poorly understood. Discrimination between these two possible sources is problematic, however, since both have large Fe, Mg, and HREE reservoirs.

Lunar Provenance and Implications

Remote sensing studies of the Moon indicate that the lunar surface is heterogeneous (Davis and Spudis 1985). A map of orbital data for the Th-Ti ratio versus Fe originally made it possible to recognize three major lunar rock types

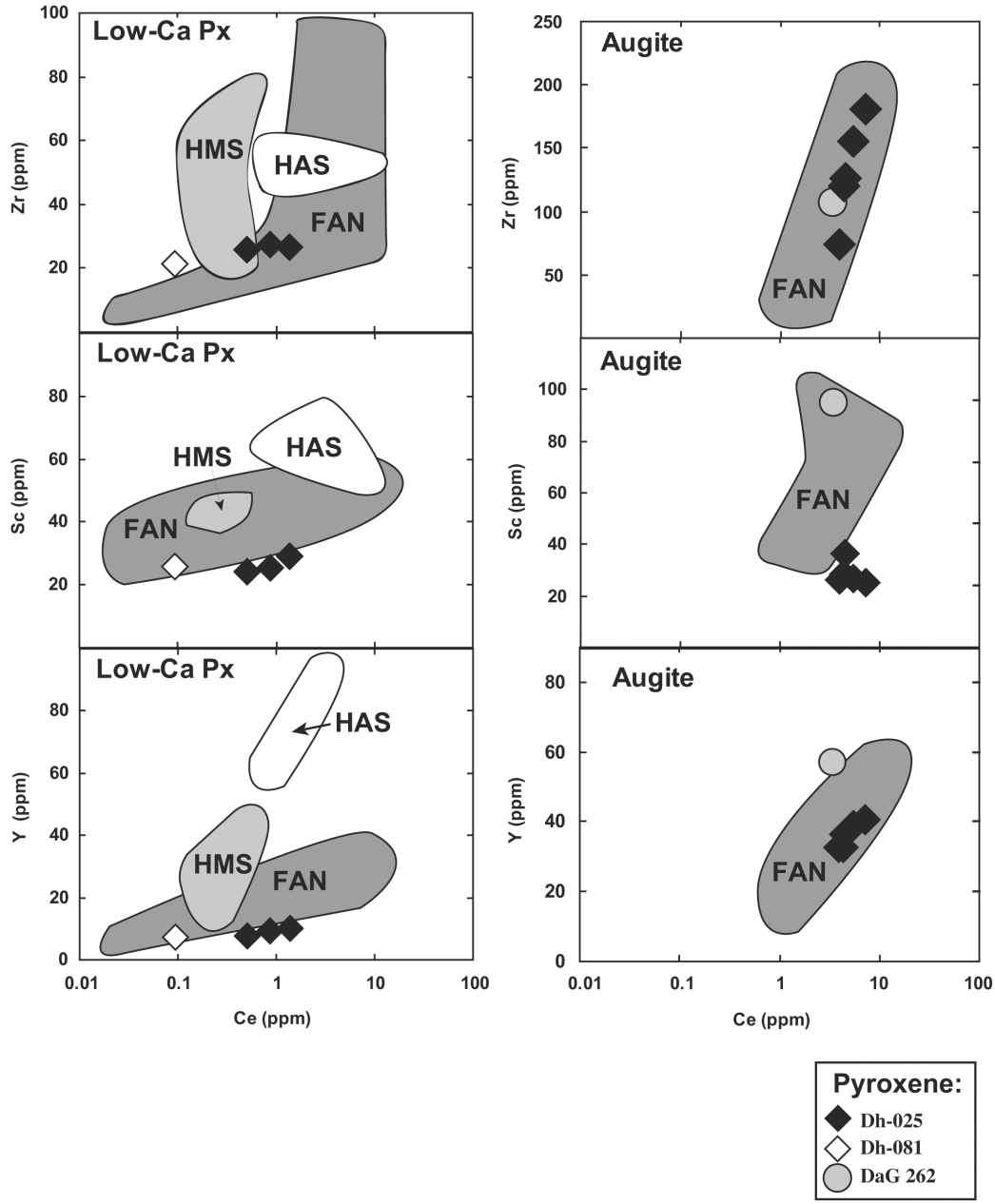

Fig. 16. Trace element concentrations of low- and high-Ca pyroxenes in the lunar meteorites Dho 025, Dho 081, and DaG 262 compared to data for typical FANs, HMS, and high-alkali suite (HAS) rocks (Floss et al. 1998; Papike et al. 1994, 1996; Papike 1996; Snyder et al. 2004).

across a large fraction of the lunar surface. These rock types are ferroan anorthosites, mare basalts, and KREEP/HMS norites. Nearly all mare basalts occur on the near side of the Moon, although a few mare terrains are seen on the far side. More recent maps generated from Clementine and Lunar Prospector data show that the bulk of the highlands are anorthositic, although petrologically heterogeneous (Spudis et al. 2000, 2002). Mare terrains also show heterogeneous characteristics with no impact basin being filled with a single type of basalt. These observations, along with the knowledge that the far side has a substantially thicker crust than the near side (86 versus 64 km) (Taylor 1982), provide a detailed view of the Moon's crustal geology.

The lunar meteorites in this study are highly anorthositic breccias with a small HMS contribution and lack KREEPy signatures. Many clasts within these breccias show a mixture of FAN and HMS chemistries but do not exhibit textures typical of lunar granulites. These characteristics represent a type of highland terrain that differs significantly from the KREEPy impact breccias that dominate the lunar collection. These rocks must have originated from a largely FAN-rich terrain, removed from appreciable HMS and KREEP influences.

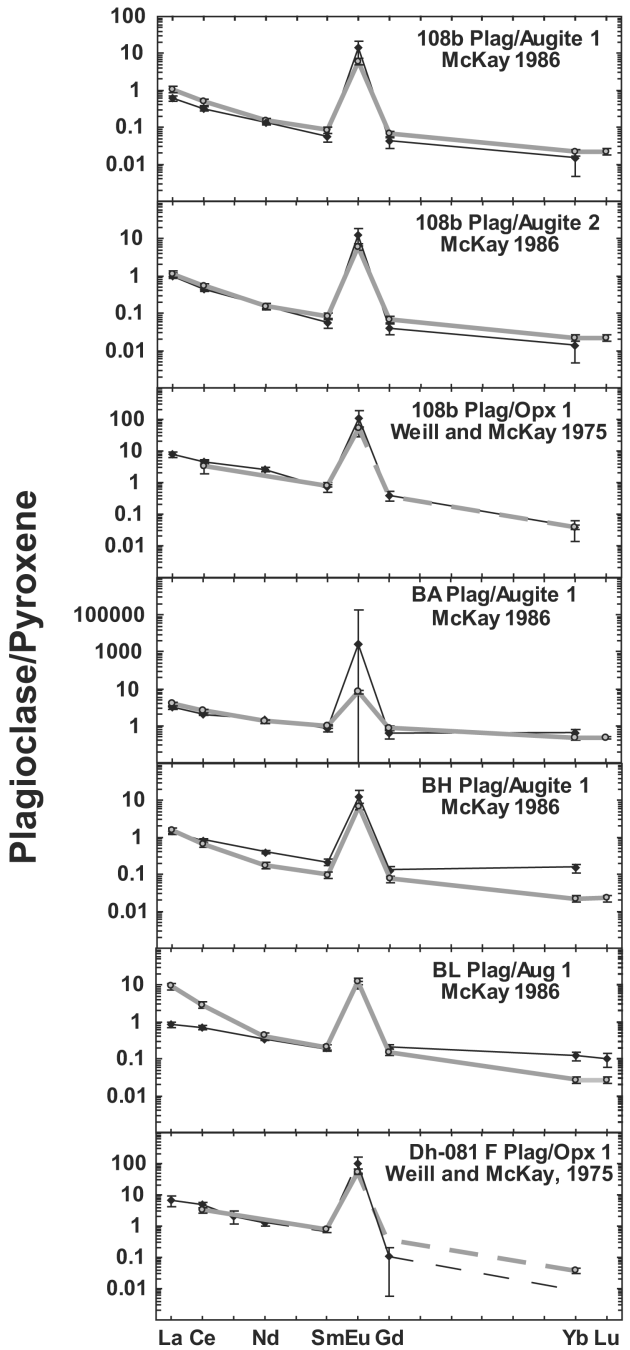

Fig. 17. Comparison of plagioclase-pyroxene REE concentration ratios and their mineral-melt distribution coefficient ratios (McKay et al. 1986, 1991; Phinney and Morrison 1990; Weill and McKay 1975). The filled diamonds and solid lines show the REE concentration ratios. The open circles and gray lines show experimentally determined distribution coefficient ratios.

On average, the highland regions on the near side of the Moon are dominated by HMS and KREEP-signatured lithologies, making an origin of these Dhofar and DaG meteorites from a terrain on the near side less likely. Nevertheless, the near side is not monolithic, and an origin on this side of the Moon cannot be completely ruled out. Norman (1981) made a detailed study of a similar set of rocks collected from the rim of North Ray crater in the Descartes Mountains. Like the lunar meteorites studied here, 67016 is also characterized by a small regolith component, low concentrations of KREEP, and similar abundances of magnesian and ferroan clast types. Thus, a near side origin for these meteorites is possible.

However, based on remote sensing data, the lunar far side is shown to be comprised almost exclusively of highland terrains with little HMS and KREEPy components. Thus, the Dhofar and DaG meteorites could also have come from the far side. Studies by Greshake et al. (1998), Bischoff et al. (1998), and Semenova et al. (2000) have reached similar conclusions.

If these meteorites are indeed from the far side, this has implications for our current view of the Moon. It suggests that FAN and HMS magmatism may be global events. One clast, with arguably pristine chemistry, occupies the FAN and HMS gap, implying that FAN and HMS magmatism may be more closely related than previously thought. Based on low concentrations of ITE, the role of KREEP in far side HMS magmatism may be less significant than on the near side. This observation is consistent with recent claims that KREEP is restricted to the western limb of the near side. And, finally, impact gardening of the lunar crust appears to have produced a widespread and ubiquitous group of mixed impactite rocks that are similar in composition to lunar granulites.

SUMMARY

The lunar meteorites Dho 025, Dho 081, DaG 262, and DaG 400 are feldspathic highlands breccias. All four meteorites consist dominantly of FAN clasts, although some Dho 025, Dho 081, and DaG 400 clast compositions plot within the FAN-HMS "gap" on a plagioclase AN versus mafic-mineral Mg# diagram (Semenova et al. 2000). All four meteorites also plot between the FAN and HMS suites in terms of whole rock Ti-Sm ratios. These "gap" fillers are dominantly mixed rocks, but REE ratios suggest that pristine lithologies may exist with FAN + HMS chemistries. SIMS analyses of single clasts from DaG and Dhofar meteorites show stronger FAN affinities than seen in whole rock data but also indicate admixture of a small (≤12% average) HMS component. Furthermore, these meteorites lack mare lithologies and the KREEPy signatures that dominate the impact breccias of previously characterized highland terrains from the lunar near side and probably represent a type of highlands terrain not previously documented in the lunar collection.

Based on a comparison of their chemistries with the remote sensing data from Clementine and Lunar Prospector, it is inferred that these rocks probably originated on the far side of the Moon; albeit, a near side origin cannot be conclusively dismissed as an option. A far side origin for these rocks has several implications for our understanding of the Moon:

- A new type of highlands terrain has been characterized that differs significantly from the KREEPy impact breccias that dominate the lunar database.
- Impact gardening of the lunar crust produces mixed rocks similar in composition to lunar granulites, and these rocks are geographically widespread.
- FAN and HMS magmatism are global events.
- The relationship between FAN and HMS magmatism may be closer than previously recognized.
- The role of KREEP assimilation in the petrogenesis of HMS rocks on the far side may be less significant than on the near side.

Acknowledgments–We would like to express our appreciation to Allan Patchen, for his help with the electron microprobe analyses. Our sincere thanks to Dr. Robert Clayton and Dr. Tosh Mayeda for their unselfish sharing of oxygen isotope data. We are also grateful to the Vernadsky Institute, the Max-Planck-Institute for Chemistry, Mainz, and the Institute for Planetology, Munster for their willingness to supply the samples necessary for this study. The graduate assistantship to J. T. Cahill from the Department of Earth and Planetary Sciences, The University of Tennessee is gratefully acknowledged. A special thanks to the Joint United States/ Russia Research in Space Sciences (JURRISS) Program (NAG 5–8726 to L. A. Taylor) sponsored by NASA. Portions of this research have also been supported by NASA grants to L. A. Taylor (NAG5–11158) and C. Floss (NAG5–13467) and a Russian Academy of Science Award to M. A. Nazarov (02–05–64981 to R.F.B.R.). Excellent reviews by Dr. Marc Norman, Dr. Ross Taylor, Dr. Hap McSween, Dr. Dan Britt, and an anonymous reviewer helped improve this manuscript and are greatly appreciated.

Editorial Handling—Dr. Ross Taylor

REFERENCES

Alexander C. M. O. D. 1994. Trace element distributions within ordinary chondrite chondrules: Implications for chondrule formation conditions and precursors. *Geochimica et Cosmochimica Acta* 58:3451–3467.

Anand M., Taylor L. A., Patchen A., Cahill J. T., and Nazarov M. A. 2002. New minerals from a new meteorite Dhofar 280. (abstract #1653). 33rd Lunar and Planetary Science Conference. CD-ROM.

Anand M., Taylor L. A., Misra K. C., Demidova S., and Nazarov M. A. 2003. KREEPy lunar meteorite Dhofar 287A: A new lunar mare basalt. *Meteoritics & Planetary Science* 38:485–499.

Anders E. and Grevesse N. 1989. Abundances of the elements: Meteoritic and solar. *Geochimica et Cosmochimica Acta* 53:197–214.

Arai T. and Warren P. H. 1999. Lunar meteorite Queen Alexandra Range 94281: Glass compositions and other evidence for launch pairing with Yamato-793274. *Meteoritics & Planetary Science* 34:209–234.

Barrat J. A., Gillet P., Lesourd M., Blichert-Toft J., and Poupeau G. R. 1999. The Tatahouine diogenite: Mineralogical and chemical effects of sixty-three years of terrestrial residence. *Meteoritics & Planetary Science* 34:91-97.

Bickel C. E. and Warner J. L. 1978. Survey of lunar plutonic and granulitic lithic fragments. Proceedings, 9th Lunar and Planetary Science Conference. pp. 629–652.

Bischoff A., Weber D., Clayton R. N., Faestermann T., Franchi I. A., Herpers U., Knie K., Korschinek G., Kubik P. W., Mayeda T. K., Merchel S., Michel R., Neumann S., Palme H., Pillinger C. T., Schultz L., Sexton A. S., Spettel B., Verchosvsky A. B., Weber H. W., Weckwerth G., and Wolf D. 1998. Petrology, chemistry, and isotopic compositions of the lunar highland regolith breccia Dar al Gani 262. *Meteoritics & Planetary Science* 33:1243–1257.

Bland P. A., Berry F. J., Smith T. B., Skinner S. J., and Pillinger C. T. 1996. The flux of meteorites to the Earth and weathering in hot desert ordinary chondrite finds. *Geochimica et Cosmochimica Acta* 60:2053–2059.

Cahill J. T., Taylor L. A., Cohen B. A., Fayek M., Riciputi L. R., and Nazarov M. A. 2001. Lunar meteorite Dhofar 025: Plagioclase REEs confirm non-pristine nature for highland clasts (abstract). *Meteoritics & Planetary Science* 36:A36.

Cahill J. T. 2003. *Petrogenesis of lunar highlands meteorites: Dhofar 025, Dhofar 081, Dar al Gani 262, and Dar al Gani 400.* Knoxville: University of Tennessee.

Clayton R. N. and Mayeda T. K. 1983. Oxygen isotopes in eucrites, shergottites, nakhlites, and chassignites. *Earth and Planetary Science Letters* 62:1–6.

Clayton R. N. and Mayeda T. K. 1996. Oxygen isotope studies of achondrites. *Geochimica et Cosmochimica Acta* 60:1999–2017.

Cohen B. A., James O. B., Taylor L. A., Nazarov M. A., and Barsukova L. D. Forthcoming. Lunar highland meteorite Dhofar 026: A strongly shocked, partially melted, granulitic breccia. *Meteoritics & Planetary Science.*

Crozaz G. and Wadhwa M. 2001. The terrestrial alteration of Saharan shergottites Dar al Gani 476 and 489: A case study of weathering in a hot desert environment. *Geochimica et Cosmochimica Acta* 65:971–978.

Crozaz G., Floss C., and Wadhwa M. 2003. Chemical alteration and REE mobilization in meteorites from hot and cold deserts. *Geochimica et Cosmochimica Acta* 67:4727–4741.

Cushing J. A., Taylor G. J., Norman M. D., and Keil K. 1999. The granulitic impactite suite: Impact melts and metamorphic breccias of the early lunar crust. *Meteoritics & Planetary Science* 34:185–195.

Davis P. A. and Spudis P. D. 1985. Petrologic province map of the lunar highlands derived from orbital geochemical data. Proceedings, 16th Lunar and Planetary Science Conference. pp. D61–D74.

Demidova S. I., Nazarov M. A., Anand M., and Taylor L. A. 2002. Lunar regolith breccia Dhofar 287B: A record of lunar volcanism. *Meteoritics & Planetary Science* 38:501–514.

Fagan T. J., Bunch T. E., Wittke J. H., Jarosewich E., Clayton R. N., Mayeda T., Eugster O., Lorenzetti S., Keil K., and Taylor G. J. 2000. Northwest Africa 032: A new lunar mare basalt (abstract). *Meteoritics & Planetary Science* 35:A51.

Fagan T. J., Keil K., Taylor G. J., Hicks T. L., Killgore M., Bunch T. E., Wittke J. H., Eugster O., Lorenzetti S., Mittlefehldt D. W., Clayton R. N., and Mayeda T. 2001. New lunar meteorite Northwest Africa 773: Dual origin by cumulate crystallization and impact brecciation (abstract #5149). 64th Annual Meteoritical Society Meeting.

Fagan T. J., Taylor G. J., Keil K., Bunch T. E., Witke J. H., Korotev R. L., Jolliff B. L., Gillis J. J., Haskin L. A., Jarosewich E., Clayton R. N., Mayeda T. K., Fernandes V. A., Burgess R.,

Turner G., Eugster O., and Lorenzetti S. 2002. Northwest Africa 032: Product of lunar volcanism. *Meteoritics & Planetary Science* 37:371–394.

Floss C., James O. B., McGee J. J., and Crozaz G. 1998. Lunar ferroan anorthosite petrogenesis: Clues from trace element distributions in FAN subgroups. *Geochimica et Cosmochimica Acta* 62:1255–1283.

Floss C. and Jolliff B. 1998. Rare earth element sensitivity factors in calcic plagioclase (anorthite). In *Secondary ion mass spectrometry: SIMS XI,* edited by Gillen G., Lareau R., Bennett J., and Stevie F. New York: John Wiley & Sons. pp. 785–788.

Floss C. and Crozaz G. 2001. Terrestrial alteration of lunar meteorites Dar al Gani 262 and 400. (abstract # 1105). 32nd Lunar and Planetary Science Conference. CD-ROM.

Grossman J. N. 2000. The meteoritical bulletin, No. 84. *Meteoritics & Planetary Science* 35:A199–A225.

Hsu W. 1995. Ion microprobe studies of the petrogenesis of enstatite chondrites and eucrites. Ph.D. thesis, Washington University, St. Louis, Missouri, USA.

Hsu W. and Crozaz G. 1996. Mineral chemistry and the petrogenesis of eucrites: I. Noncumulate eucrites. *Geochimica et Cosmochimica Acta* 60:4571–4591.

Hsu W. and Crozaz G. 1997. Mineral chemistry and the petrogenesis of eucrites: II. Cumulate eucrites. *Geochimica et Cosmochimica Acta* 61:1293–1302.

James O. B., Floss C., and McGee J. J. 2002. Rare earth element variations resulting from inversion of pigeonite and subsolidus reequilibration in lunar ferroan anorthosites. *Geochimica et Cosmochimica Acta* 65:1269–1284.

Jolliff B. L., Korotev R. L., and Haskin L. A. 1991. A ferroan region of the lunar highlands as recorded in meteorites MAC 88104 and MAC 88105. *Geochimica et Cosmochimica Acta* 55:3051–3071.

Jolliff B. L. and Haskin L. A. 1995. Cogenetic rock fragments from a lunar soil: Evidence of a ferroan noritic-anorthosite pluton on the Moon. *Geochimica et Cosmochimica Acta* 59:2345–2374.

Jolliff B. L., Korotev R. L., and Rockow K. M. 1998. Geochemistry and petrology of lunar meteorite Queen Alexandra Range 94281, a mixed mare and highland regolith breccia, with special emphasis on very-low-titanium mafic components. *Meteoritics & Planetary Science* 33:581–601.

Jolliff B. L., Korotev R., and Arnold S. 1999. Electron microprobe analyses of Dar al Gani lunar meteorite, a sample of the feldspathic highlands terrane of the moon. (abstract #2000). 29th Lunar and Planetary Science Conference. CD-ROM.

Kaiden H. and Kojima H. 2002. Yamato-983885: A new lunar meteorite found in Antarctica. (abstract #1958). 33rd Lunar and Planetary Science Conference. CD-ROM.

Koeberl C., Kurat G., and Brandstatter F. 1991a. MAC 88105—A regolith breccia from the lunar highlands: Mineralogical, petrological, and geochemical studies. *Geochimica et Cosmochimica Acta* 55:3073–3087.

Koeberl C. K., Kurat G., and Brandstatter F. 1991b. Lunar meteorite Yamato-793274: Mixture of mare and highland components, and baringerite from the Moon. *Proceedings of the NIPR Symposium on Antarctic Meteorites* 4:33–55.

Kojima H. and Imae N. 2001. New lunar meteorite: Yamato-983885 *Meteorite Newsletter* 10:1.

Korotev R. 1994. Compositional variation in Apollo 16 impact-melt breccias and inferences for the geology and bombardment histroy of the Central Highlands of the Moon. *Geochimica et Cosmochimica Acta* 58:3931–3969.

Korotev R., Jolliff B. L., and Rockow K. M. 1996. Lunar meteorite Queen Alexandra Range 93069 and the iron concentration of the lunar highlands surface. *Meteoritics & Planetary Science* 31: 909–924.

Korotev R. 1997. Some things we can infer about the Moon from the composition of the Apollo 16 regolith. *Meteoritics & Planetary Science* 32:447–478.

Laul J. C., Wakita H., Showalter D. L., Boynton W. V., and Schmitt R. A. 1972. Bulk rare earth and other trace elements in Apollo 14 and 15 and Luna 16 samples. Proceedings, 3rd Lunar and Planetary Science Conference. pp. 1181–1200.

Lindstrom M., Marvin U. B., Holmber B. B., and Mittlefehldt D. W. 1990. Apollo 15 KREEP-poor impact melts. Proceedings, 20th Lunar and Planetary Science Conference. pp. 77–90.

Lindstrom M. M. and Lindstrom D. J. 1986. Lunar granulites and their precursor anorthositic norites of the early lunar crust. Proceedings, 17th Lunar and Planetary Science Conference. pp. D263–276.

Lindstrom M. M., Mittlefehldt D. W., Martinez R. R., Lipschutz M. E., and Wang M. S. 1991. Geochemistry of Yamato-82192, -86032 and -793274 lunar meteorites. P*roceedings of the NIPR Symposium on Antarctic Meteorites* 4:12–32.

Longhi J. and Boudreau A. E. 1979. Complex igneous processes and the formation of primitive lunar crustal rocks. Proceedings, 10th Lunar and Planetary Science Conference. pp. 2085–2105.

McKay G., Wagstaff J., and Yang S. R. 1986. Clinopyroxene REE distribution coefficients for shergottites: The REE content of the Shergotty melt. *Geochimica et Cosmochimica Acta* 50:927–937.

McKay G., Le L., and Wagstaff J. 1991. Constraints on the origin of the mare basalt europium anomaly: REE partitioning coefficients for pigeonite (abstract). Proceedings, 22nd Lunar and Planetary Science Conference. pp. 883–884.

McKay G. A. 1982. Partitioning of REE between olivine, plagioclase, and synthetic basaltic melts: Implications for the origin of lunar anorthosites. Proceedings, 13th Lunar and Planetary Science Conference. pp. 493–494.

McKay G. A. 1989. Partitioning of rare earth elements between major silicate minerals and basaltic melts. In *Geochemistry and mineralogy of rare earth elements,* edited by Lipin B. R. and McKay G. A. Washington D.C.: Mineralogical Society of America. pp. 45–77.

Nazarov M. A., Demidova S. I., Patchen A., and Taylor L. A. 2002. Dhofar 301, 302, and 303: Three new lunar highland meteorites from Oman. (abstract #1293). 33rd Lunar and Planetary Science Conference. CD-ROM.

Neal C. R., Taylor L. A., Liu Y., and Schmitt R. A. 1991. Paired lunar meteorites MAC 88104 and MAC 88105: A new "FAN" of lunar petrology. *Geochimica et Cosmochimica Acta* 55:3037–3049.

Nishiizumi K., Okazaki R., Park J., Nagao K., Masarik J., and Finkel R. C. 2002. Exposure and terrestrial histories of Dhofar 019 martian meteorite. (abstract #1366). 33rd Lunar and Planetary Science Conference. CD-ROM.

Norman M. D. and Ryder G. 1980. Geochemical constraints on the igneous evolution of the lunar crust. Proceedings 11th Lunar and Planetary Science Conference. pp. 317–331.

Norman M. D. 1981. Petrology of suevitic lunar breccia 67016. Proceedings, 12th Lunar and Planetary Science Conference. pp. 235–252.

Palme H., Spettel B., Jochum K. P., Dreibus G., Weber H., Weckwerth G., Wonke H., Bishoff A., and Stöffler D. 1991. Lunar highland meteorites and the composition of the lunar crust. *Geochimica et Cosmochimica Acta* 55:3105–3122.

Papike J. J., Fowler G. W., and Shearer C. K. 1994. Orthopyroxene as a recorder of lunar crust evolution: An ion microprobe investigation of Mg-suite norites. *American Mineralogist* 79: 796–800.

Papike J. J. 1996. Pyroxene as a recorder of cumulate formational processes in asteroids, Moon, Mars, Earth: Reading the record with the ion microprobe. *American Mineralogist* 81:525–544.

Papike J. J., Fowler G. W., and Shearer C. K. 1996. Ion microprobe investigation of plagioclase and orthopyroxene from lunar Mg-suite norites: Implications for calculating parental melt REE concentrations and for assessing post crystallization REE redistribution. *Geochimica et Cosmochimica Acta* 60:3967–3978.

Papike J. J., Fowler G. W., and Shearer C. K. 1997. Evolution of the lunar crust: SIMS study of plagioclase from ferroan anorthosites. *Geochimica et Cosmochimica Acta* 61:2343–2350.

Papike J. J. 1998. Comparative planetary mineralogy: Chemistry of melt-derived pyroxene, feldspar, and olivine. In *Planetary materials,* edited by Papike J. J. Washington D.C.: Mineralogical Society of America. pp. 1–11.

Papike J. J., Karner J. M., and Shearer C. K. 2003. Determination of planetary basalt parentage: A simple technique using the electron microprobe. *American Mineralogist* 88:469–472.

Phinney W. C. and Morrison D. A. 1990. Partition coefficients for calcic plagioclase: Implications for Archean anorthosites. *Geochimica et Cosmochimica Acta* 54:1639–1654.

Pieters C. M. 1978. Mare basalt types on the front side of the Moon: A summary of spectral reflectance data. Proceedings, 9th Lunar and Planetary Science Conference. pp. 2825–2849.

Semenova A. S., Nazarov M. A., Konokova N. N., Patchen A., and Taylor L. A. 2000. Mineral chemistry of lunar meteorite Dar al Gani 400. (abstract #1252). 31st Lunar and Planetary Science Conference. CD-ROM.

Shervais J. W., Taylor L. A., and Lindstrom M. M. 1997. 28th Lunar and Planetary Science Conference. pp. 1301–1302.

Shervais J. W. and McGee J. J. 1998a. Ion and electron microprobe study of troctolites, norite, and anorthosites from Apollo 14: Evidence for urKREEP assimilation during petrogenesis of Apollo 14 Mg-suite rocks. *Geochimica et Cosmochimica Acta* 62:3009–3023.

Shervais J. W. and McGee J. J. 1998b. KREEP in the western lunar highlands: Ion and electron microprobe study of alkali suite anorthosites and norites from Apollo 12 and 14. *American Mineralogist* 84:806–820.

Shervais J. W. and McGee J. J. 1999. KREEP cumulates in the western lunar highlands: Ion and electron microprobe study of alkali-suite anorthosites and norites from Apollo 12 and 14. *American Mineralogist* 84:806–820.

Snyder G. A., Neal C. R., Ruzicka A. M., and Taylor L. A. 1999. Lunar meteorite EET 96008, Part II: Whole rock trace element and PGE chemistry and pairing with EET 87521. (abstract #1705). 30th Lunar and Planetary Science Conference. CD-ROM.

Snyder G. A., Floss C., Crozaz G., and Taylor L. A. Forthcoming. Probing the crust of the Earth's moon: Trace elements in minerals from post magama-ocean, highland rocks. *Meteoritics & Planetary Science.*

Spettel B., Dreibus G., Burghele A., Jochum K. P., Schultz L., Weber H. W., Wlotzka F., and Wanke H. 1995. Chemistry, petrology, and noble gases of lunar highland meteorite Queen Alexandra Range 93069 (abstract). *Meteoritics* 30:583.

Spudis P. D., Bussey D. B. J., and Gillus J. 2000. Petrologic mapping of the Moon from Clementine and Lunar Prospector Data: Incorporation of new thorium data. (abstract #1414). 31st Lunar and Planetary Science Conference. CD-ROM.

Spudis P. D., Zellner N., Delano J., Whittet D. C. B., and Fessler B. 2002. Petrologic mapping of the Moon: A new approach. (abstract #1104). 33rd Lunar and Planetary Science Conference. CD-ROM.

Stelzner T. H., Heide K., Bishchoff A., Weber D., Schultz L., Happel M., Schron W., Neuper U., Michel R., Clayton R. N., Mayeda T. K., Bonani G., Haidas I., Ivy-Ochs S., and Suter M. 1999. An interdisciplinary study of weathering effects in ordinary chondrites from the Acfer region. *Meteoritics & Planetary Science* 34:787–794.

Stöffler D. and Knöll H.-D. 1977. Composition and origin of plagioclase, pyroxene, and olivine clasts of lunar breccias 14006, 14063, 14066, 14311, 14320, and 14321. Proceedings, 8th Lunar Science Conference. pp. 1849–1867.

Taylor L. A., Nazarov M. A., Cohen B. A., Warren P. H., Barsukova L. D., Clayton R. N., and Mayeda T. K. 2001. Bulk chemistry and oxygen isotopic compositions of lunar meteorites Dhofar 025 and Dhofar 026. (abstract #1985). 32nd Lunar and Planetary Science Conference. CD-ROM.

Taylor S. R. 1982. *Planetary science: A lunar perspective.* Houson: Lunar and Planetary Institute. 481 p.

Treiman A. H. 1996. The perils of partition: Difficulties in retrieving magma compositions from chemically equilibrated basaltic meteorites. *Geochimica et Cosmochimica Acta* 60:147–155.

Warren P. H. and Wasson J. T. 1980. Further foraging for pristine nonmare rocks: Correlations between geochemistry and longitude. Proceedings, 11th Lunar and Planetary Science Conference. pp. 431–470.

Warren P. H. 1985. The magma ocean concept and lunar evolution. *Annual Review of Earth and Planetary Sciences* 13:201–240.

Warren P. H. and Kallemeyn G. W. 1989. Elephant Moraine 87521: The first lunar meteorite composed of predominantly mare material. *Geochimica et Cosmochimica Acta* 53:3323–3330.

Warren P. H. and Kallymeyn G. W. 1991. The MacAlpine Hills lunar meteorite and implications of the lunar meteorites collectively for the composition and origin of the Moon. *Geochimica et Cosmochimica Acta* 55:3123–3138.

Warren P. H. 1993. A concise compilation of petrologic information on possibly pristine nonmare Moon rocks. *American Mineralogist* 78:360–376.

Warren P. H. and Kallemeyn G. W. 1993. Geochemical investigation of two lunar mare meteorites: Yamato-793169 and Asuka-881757. *Proceedings of the NIPR Symposium on Antarctic Meteorites* 6:35–37.

Warren P. H., Taylor L. A., Kallemeyn G., Cohen B. A., and Nazarov M. A. 2001. Bulk compositional study of three Dhofar lunar meteorites: Enigmatic siderophile element results for Dhofar 026. (abstract #2197). 32nd Lunar and Planetary Science Conference. CD-ROM.

Weill D. G. and McKay G. A. 1975. The partitioning of magnesium, iron, strontium, cerium, samarium, europium, and ytterbium in lunar igneous systems and a possible origin of KREEP by equilibrium partial melting. Proceedings, 11th Lunar and Planetary Science Conference. pp. 1143–1158.

Wiechert U., Halliday A. N., Lee D. C., Snyder G. A., Taylor L. A., and Bumble D. 2001. Oxygen isotopes and the Moon-forming giant impact. *Science* 294:345–348.

Zinner E. and Crozaz G. 1986a. A method for the quantitative measurement of rare earth elements in the ion microprobe. *International Journal of Mass Spectrometry and Ion Processes* 69:17–38.

Zinner E. and Crozaz G. 1986b. Ion probe determination of the abundances of all the rare earth elements in single mineral grains. In *Secondary ion mass spectrometry, SIMS V,* edited by Colton R. J. New York: Springer Verlag. pp. 444–446.

Zipfel J., Spettel B., Palme H., Wolf D., Franchi I., Sexton A. S., Pillinger C. T., and Bischoff A. 1998. Dar al Gani 400: Chemistry and petrology of the largest lunar meteorite (abstract). *Meteoritics & Planetary Science* 33:A171.

APPENDIX

Table A1. Summary of petrographic classifications and mineral compositions of Dho 025 and Dho 081 clasts.[a]

Sample	Rock	Plagioclase	Olivine	Pyroxene			
Dho 025	Textural type	An	Fo	Wo	En	Fs	Mg#
AA	LC	96.6–97.3	75.1–77.8				
AB	LC	96.9–98.0	80.2–82.0				
AF	LC	95.9–96.9	69.2–73.2				
AI	LC	96.1–97.5	78.9–80.3				
A	LC	96.7	72				
B	LC	96.6	72				
K	LC	97.2	75				
T	LC	97	75				
V	LC	95.9	72				
Y	LC	97	64				
AC	LC	96.0–96.8		5.66–8.91	67.0–70.5	23.2–25.8	72.2–74.9
AD	LC	95.6–96.4	66.7–69.7				
AE	LC	94.2–96.1	65.1–68.7	4.53–5.36	68.8–69.5	25.9–26.1	72.6–72.9
AG	LC	95.1–96.9		33.0–38.2	47.0–50.4	14.1–16.0	75.9– 77.1
AH	LC	96.4–97.1	80.8–81.5				
BA	LC	95.6–96.9		3.30–4.41	75.2–76.5	19.6–20.4	79
	LC			39.3–44.4	46.7– 50.0	8.9–10.7	81.5–83.4
BB	LC	96.9–97.6	74.1– 82.1				
BC	LC	95.1–98.0		8.04–15.3	56.4–66.0	22.1–31.1	65.5–75.2
BD	LC	96.6–97.5		4.9– 9.6	54.9–60.4	28.2–37.1	58.9–68.8
	LC			38.3–40.3	41.3–43.3	18.0–19.6	70
BF	LC	94.7–97.9		8.30–14.6	58.6–67.3	22.8–31.0	65.7–74.5
BH	LC	96.4–97.0		3.66– 7.08	73.6–77.8	17.4–19.3	81
	LC			37.4– 41.8	46.6–48.2	10.0–12.3	81
BL	LC	95.7–96.7	69.9–73.2	38.2–44.3	45.6–49.9	9.3–15.3	79
BM	LC	96.0–97.1	77.5–82.7	2.91–6.40	78.5–81.7	15.2–16.8	83
BO	LC	96.1–97.0	71.4–73.0				
BP	LC	95.6–96.3	70.6–72.5				
25.8	LC	90.6–92.9	89	5.90–7.74	81.7–83.4	10.5–10.7	88
78	LC	94.2–96.9	68.0–73.3	6.31–10.8	66.0–69.2	23.1–24.5	73.8–74.5
				34.9–39.5	47.0–50.4	13.9–14.7	77.4– 77.8
93	LC	95.2–97.5	76.4–80.7	2.73–8.38	70.3–80.6	15.5–17.2	82.5
108b	LC	95.6–95.9		3.26–3.77	79.3–79.9	16.6–17.1	82
				39.5–44.5	46.6–50.1	8.77–11.2	82
Troc1	LC	96.4	81				
Troc3	LC	96.7	72				
Troc4	LC	96.4	72				
Gran1	GR	96.5	79				
BE	MF			20.8–37.8	45.1–55.4	15.2–23.9	67.5–75.8
BG	MF			12.7–21.4	52.3–58.7	25.8–30.4	65.2–69.2
BI	MF	95.3–96.1					
BK	MF			3.4–4.6	72.1– 73.1	23.3–23.6	75
				40.4–43.4	45.3–47.1	11.1–13.4	76.5–80.7
71a	MF			5.51–9.94	54.8–61.9	29.0–37.5	60.8–68.1
71b	MF			4.46–9.28	58.9–64.1	28.0–36.5	61.8–69.6
71c	MF		75.2–81.5				
74	MF			4.43–10.3	66.5–72.5	22.7–24.6	74.2–76.5
108	MF			28.7–37.5	34.5–46.7	24.8–32.5	51.5–65.2
121.1	MF			9.03–12.2	56.3–61.8	27.4–33.6	62.4–68.4
121.2	MF		70.7–81.6				
123.1	MF			37.4–42.8	44.0–47.8	13.2–15.0	75.7–77.1
123.2	MF		72.5–77.7				
126.1	MF			6.05–8.97	56.7–64.3	29.8–34.3	57.7–68.4
126.2	MF		77.9–83.2				

Table A1. Summary of petrographic classifications and mineral compositions of Dho 025 and Dho 081 clasts.[a]

Sample	Rock	Plagioclase	Olivine	Pyroxene			
Dho 025	Textural type	An	Fo	Wo	En	Fs	Mg#
126.3	MF		79.7–82.0				
130.1	MF			9.20–13.1	58.5–66.0	25.4–31.4	65.1–71.5
130.2	MF		73.1–74.4				
C	LC	96.8–97.5	56.7–75.4				
F	LC	97.8–97.0		3.8–4.1	70.0–70.5	25.4–26.0	72.9–73.5
H	LC	96.4–98.1		5.93–9.63	71.2–75.6	18.3–21.9	76.9–80.5
I	LC	96.7–97.6	76.0–78.5				
I2	LC	96.1–97.4	74.3–79.4				
L	LC	95.4–97.4	71.0–74.4				
		95.4–97.4	72.4–81.0				
		95.4–97.4	69.8–82.0				
R	LC	95.1–97.4		39.9–40.6	32.1–32.4	27.2–27.8	53.8–54.1
				27.2–30.3	40.5	29.2–32.3	55.7–58.0
V	LC	97.3–97.5		26.5–28.8	39.2–45.5	28.0–32.1	55.0–61.9
AE	LC	92.8–97.3	81.2–83.9				
G	GR	96.0–97.0	67.7–74.1				
AF	GR	95.8–96.1	64.1–76.1				
B	MF	96.0–96.9					
D	MF	97.0–96.8					
E	MF	96.4–97.4					
H1	MF			30.1–40.4	42.0–51.9	11.4–27.9	60.1–81.8
J	MF		50.2–74.1	19.6–25.3	25.8–32.1	42.6–52.9	32.7–43.0
K	MF	95.3–97.7					
K1	MF		71.2–81.6				
M	MF	96.4–97.3					
O	MF	96.7– 97.7					
P	MF	96.7–97.2					
Q	MF	94.8–96.5					
T	MF		59.0–70.5				
V1	MF			12.6–24.9	49.4–62.8	21.3–25.7	65.8–74.7
V2	MF		81.2–84.9	39.4–42.4	38.1– 46.3	14.3–19.4	66.2–76.4
W	MF	97.1–97.7					
W1	MF		80.7–82.6	3.62–5.21	62.1–64.4	30.4–34.3	64.4–67.9
X	MF	96.4–97.0					
Y	MF	97.2–97.7					
Z	MF	96.0–97.4					
AC	MF	96.0–96.8					
AI	MF	97.1–97.7					

[a]Abbreviations: LC = Lithic clast; MF = Mineral fragment; GR = Granulite rocklet. Clasts with two pyroxenes are organized so that low-Ca pyroxene is listed first, followed by high-Ca pyroxene.